RESEARCH ARTICLE | SEPTEMBER 23 2020

Introductory guide to backgrounds in XPS spectra and their impact on determining peak intensities

Mark H. Engelhard; Donald R. Baer; Alberto Herrera-Gomez; ... et. al

Journal of Vacuum Science & Technology A 38, 063203 (2020)
https://doi.org/10.1116/6.0000359

View Online

Export Citation

CrossMark

Related Content

Three-dimensional spectral proper orthogonal decomposition analyses of the turbulent flow around a seal-vibrissa-shaped cylinder

Physics of Fluids (February 2021)

Interface energetics at WO_X/organic interfaces: The role of oxygen vacancies

Appl. Phys. Lett. (September 2013)

Study of W/WC Coatings Varying the Substrate Temperature

AIP Conference Proceedings (December 2006)

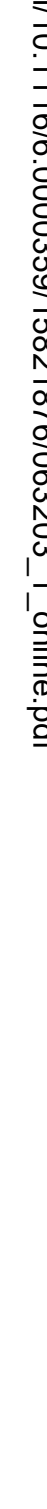
Downloaded from http://pubs.aip.org/avs/jva/article-pdf/doi/10.1116/6.0000359/15821876/063203_1_online.pdf

JVST A
Journal of Vacuum Science & Technology A

ARTICLE

avs.scitation.org/journal/jva

Introductory guide to backgrounds in XPS spectra and their impact on determining peak intensities

Cite as: J. Vac. Sci. Technol. A **38**, 063203 (2020); doi: 10.1116/6.0000359
Submitted: 27 May 2020 · Accepted: 31 August 2020 ·
Published Online: 23 September 2020

View Online

Export Citation

CrossMark

Mark H. Engelhard,[1,a)] Donald R. Baer,[1] Alberto Herrera-Gomez,[2] and Peter M. A. Sherwood[3]

AFFILIATIONS

[1]Environmental Molecular Sciences Laboratory, Pacific Northwest National Laboratory, Richland, Washington 99354
[2]CINVESTAV—Unidad Queretaro, Queretaro 76230, Mexico
[3]Department of Chemistry, University of Washington, Box 351700, Seattle, Washington 98195

Note: This paper is part of the Special Topic Collection on Reproducibility Challenges and Solutions.
[a)]**Electronic mail:** mark.engelhard@pnnl.gov

ABSTRACT

Photoelectron and Auger peaks are central to most of the important uses of x-ray photoelectron spectroscopy (XPS), and thus, they receive the most attention in many types of analysis. Quantitative chemical analysis using XPS requires the assessment of the intensities of the photoemission *peaks* of the elements detected. Determination of peak intensities requires separation of the photoelectron peak signals from the background on which the peaks rest. For the determination of peak area intensities, the background is subtracted from overall signal intensity. The spectral background is also critical when peak fitting is used to determine intensities of overlapping peaks, and the model of background used in this process can impact the results. In addition to the impact on quantitative analysis, information about the depth distribution of elements in the near surface region can often be obtained by visual inspection of the background and quantified using appropriate modeling. This introductory guide provides some basic information about backgrounds in the XPS analysis, describes the types of background models that are commonly used, suggests some of their strengths and weaknesses, and provides examples of their use and misuse. Although the fundamental nature of some components of the background signals in XPS is not understood, indicating that none of the models in use are fully correct and the area is subject to active research, appropriate good practices have been established for most routine analysis. The guide describes good practices, identifies errors that frequently appear in the literature, and uses examples to demonstrate the impacts of background selections on determinations of peak intensities.

Published under license by AVS. https://doi.org/10.1116/6.0000359

I. INTRODUCTION

The spectrum collected during an x-ray photoelectron spectroscopy (XPS) measurement consists of the number of electrons detected as a function of kinetic energy (KE) but usually converted and plotted on a binding energy scale (BE). The appearance of the background depends on whether the spectrum is obtained in FAT (CAE) [fixed analyzer transmission (constant analyzer energy)] or FRR (CRR) [fixed retardation ratio (constant retardation ratio)] modes. In the FAT mode, transmission is constant throughout the energy range and the background from the many electrons that have suffered energy loss increases with increasing binding energy. In the FRR mode, transmission decreases with increasing binding energy, lowering the high electron background at high binding energies (lower kinetic energies).[1] The survey wide scan spectrum in Fig. 1 used the FRR mode, while the survey shown in Fig. 3 used the FAT mode. The FAT mode is the commonly used mode today.

The peaks detected are from photoelectrons emitted from the photoemission process and Auger electrons emitted during a core-hole decay process. In addition to these photoelectron and Auger peaks, there is a spectral background. These background electrons have several sources including photo and Auger electrons that have lost their core level energy due to inelastic scattering, often coming from deep within the sample, secondary electron cascades, and possibly electrons emitted by other photon sources such as by x-ray satellites or bremsstrahlung radiation when achromatic radiation is used. Much information about a sample can be obtained from such wide scan survey data, including the identification of elements and energy ranges, important if any high-energy resolution data are to be collected.

Downloaded from http://pubs.aip.org/avs/jva/article-pdf/doi/10.1116/6.0000359/15821876/063203_1_online.pdf

Published under license by AVS.

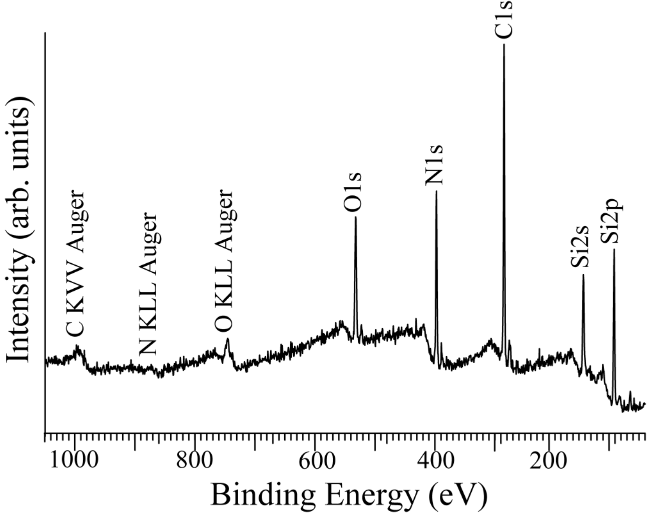

FIG. 1. Survey wide scan spectrum, collected in the FRR mode, of a silicon nitride coated carbon fiber obtained with achromatic Mg Kα X-radiation. The electrons counted between these peaks are most commonly considered background signal, although there is background within the peaks as well. The measured KE has been converted to BE using BE = hν − KE − wf_s, where hν is the x-ray energy and wf_s is the work function of the spectrometer.

The wide scan survey spectrum in the FRR mode for an untreated and unsized carbon fiber with a surface coating of silicon nitride produced by chemical vapor deposition (CVD) is shown in Fig. 1 (Ref. 2). The spectrum was obtained with a Kratos ES200B spectrometer using achromatic Mg Kα X-radiation. The spectrum shows the N 1s and Si 2s and Si 2p core XPS regions associated with Si_3N_4 and a C 1s region associated with surface hydrocarbon from the CVD process and the graphitic carbon of the underlying fiber partly exposed by cracks in the silicon nitride film. The O 1s region comes from some SiO_2 arising from the CVD process. CKVV, NKLL, and OKLL Auger features are also seen. Low intensity x-ray satellite features (discussed in Appendix B) can be seen to lower binding energy of the C 1s, N 1s, and O 1s peaks. Silicon nitride is an insulator with a 5 eV bandgap. There is good electrical contact with the carbon fiber that is grounded so no differential sample charging effects are seen.[3] The core XPS regions are shown in Fig. 2.

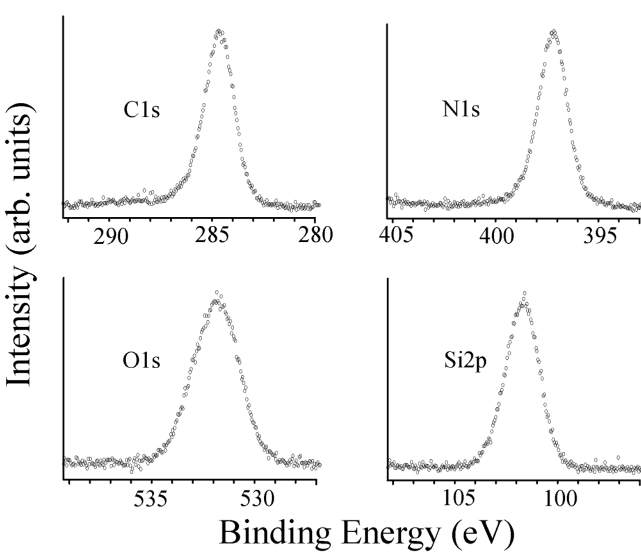

FIG. 2. XPS narrow scan of the C1 s, N1 s, O1 s, and Si2p regions of a silicon nitride coated carbon fiber.

The spectra in Fig. 2 are the unaltered experimental data with a linear horizontal background removed from all these peaks. Since the spectral regions are narrow, the FRR method of data collection has no significant difference in transmission across the spectrum.

The background that we are now concerned with is how different the background counts are across the spectral region. Figure 2 shows very little difference in the background across the spectrum for all four regions, so a linear sloping (in these cases very little slope) would give a reasonably accurate value for the areas under the peaks. There are many cases of nontransition metal compounds that display such simple backgrounds, but for many compounds, especially transition metal compounds and samples with overlayers, the background is complex and requires appropriate background models to extract useful information from the data.

The wide scan survey spectrum from TiO_2 powder is shown in Fig. 3. This spectrum is more complex than Fig. 1; it corresponds to a transition metal compound and has more features. FAT, rather than FRR, was used leading to a constant transmission function across the spectrum. There is a flat region between a binding energy of 450 eV to about 60 eV but considerable variations in the background are seen at binding energies greater than 450 eV. The background increases in moving from lower to higher binding energies (higher to lower kinetic energies) in Fig. 3.

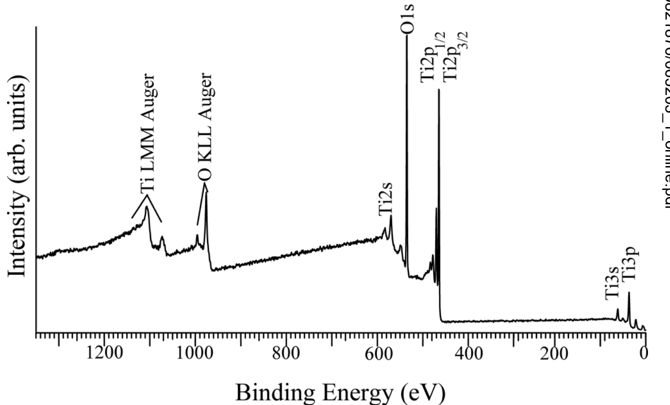

FIG. 3. XPS survey wide scan spectrum of anatase TiO_2 powder, collected in the FAT mode, obtained with monochromatic AlKα X-radiation. Photoelectron peaks are observed from Ti [3 s, 3p, 2p, 2 s] and O [1 s] along with Auger peaks [O KLL and Ti LMM].

Downloaded from http://pubs.aip.org/avs/jva/article-pdf/doi/10.1116/6.0000359/15821876/063203_1_online.pdf

Published under license by AVS.

The Ti 2p and O 1s photoelectron peaks sit on top of a relatively flat background that appears at lower BE. In addition to the photoelectron peaks, there is a significant change in the background associated with these peaks that is clearly visible on the higher BE side of the peaks. Some of the processes contributing to the background are understood, but others are subject to ongoing study.[4] To analyze the Ti 2p spectrum, both backgrounds, the flat background and the background associated with the peak, need to be removed or considered during the XPS analysis, but it is the background associated directly with the photoelectron peaks that introduce some complexity.[5]

Although important information is contained within what we call the background signal,[6,7] much of the attention during the XPS analysis is usually focused on the energy, shape, and intensity of the photoelectron or Auger peaks. For many types of analysis, including intensity determination for quantification and fitting of peaks to determine the binding energies or peak intensities of overlapping photoelectron peaks, it is important to separate the peaks from the associated background. If the objective is primarily the determination of peak intensity for quantitative analysis, it is common to subtract some type of background from the spectrum and sum the remaining counts to obtain peak intensity.[8] If peak fitting is required, some type of background is involved in the fitting process.[9] This is often influenced and sometimes constrained by the analysis software available on an XPS spectrometer or otherwise available to an analyst.

Throughout the approximately 50-year history of XPS the importance of appropriate modeling of the background signals for quantitative analysis has been recognized.[9,10] Although many approaches to modeling backgrounds have been developed,[11,12] a relatively small number of background models are used for most routine analyses. These include linear background, some version of what has been called a Shirley background and/or a version of the background developed by Tougaard. These are discussed in Sec. III. For careful studies, the nature of spectral backgrounds is very important, and a variety of sophisticated models and advanced software packages can enable more detailed analysis.[7–9] The variety of background models reported in the literature suggests a degree of discomfort some analysts feel regarding those most commonly used.[13] Because some aspects of spectral backgrounds are not understood, there is no fundamentally correct procedure to remove backgrounds in XPS spectra, making it particularly important to describe the approach and details of the background applied in a study. Published studies show comparisons of the most popular background removal procedures.[10,14–16]

This introductory guide is intended to provide some basic information about the nature of backgrounds in XPS spectra. The guide first describes the types of commonly applied background models, indicating some of their strengths and weaknesses, and then demonstrates impacts of background selection on relative peak intensities by showing examples of their use and misuse. Some aspects of components of the background signals in XPS are not understood, and so none of the models in common use are fully correct; however, consistent good practices useful for routine analysis, as well as common errors, are described.

This guide to XPS background signals is part of a collection of papers related to reproducibility, many with a focus on XPS analysis, and describes good practices and identifies errors that frequently appear in the literature. Because backgrounds are an essential part of the XPS analysis, they are also discussed in several other papers in the Reproducibility Challenges and Solutions collection of papers including those associated with quantitative analysis,[17,18] peak fitting,[19] and the associated uncertainties,[20] guides to XPS measurements on polymers[21] and nanoparticles,[22] and examples of reproducibility issues from semiconductor technology.[23]

II. USEFUL INFORMATION ABOUT BACKGROUNDS AND PHOTOELECTRON PEAKS

Some additional information about behaviors and properties of both background signals and photoelectron peaks may be helpful when considering how to extract peak intensities and other information.

A. Background shape depends on initial core level and elemental distribution

The Cr 3s and 3p photoelectron peaks shown in Fig. 4 (Ref. 4) highlight that differences can be observed in photoelectron peak background shapes for photoelectron peaks arising from different core levels of the same element. While the background for Cr 3p is

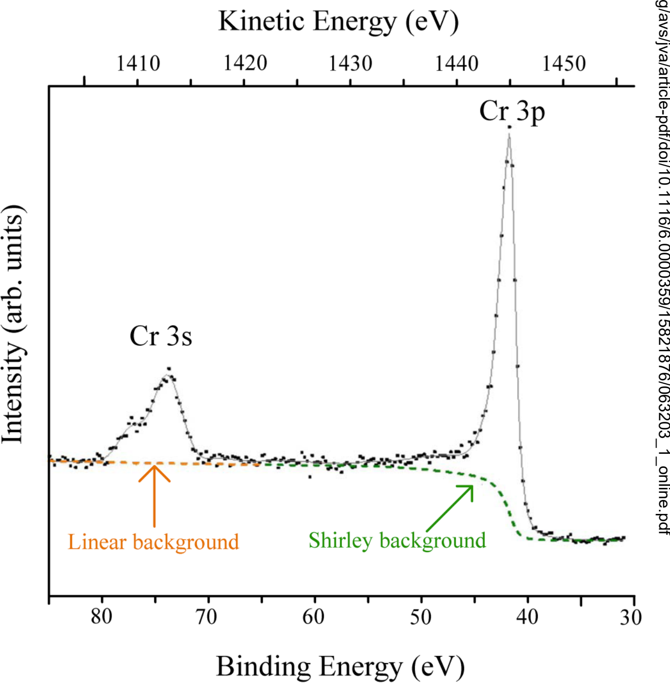

FIG. 4. Cr 3*s* and 3*p* spectra from metallic chromium acquired with a laboratory XPS equipment. The kinetic energy of both peaks, which is indicated in the top axis, is very similar between the two peaks. However, the background shape for the Cr 3*s* and 3*p* peaks is very different from each other and requires different model backgrounds. The origin of these differences is subject to current research (Ref. 4).

Downloaded from http://pubs.aip.org/avs/jva/article-pdf/doi/10.1116/6.0000359/15821876/063203_1_online.pdf

Published under license by AVS.

step shaped (which, as described later, is commonly fit by a Shirley type background), that for Cr 3s is almost a straight line. Clearly, modeling of these backgrounds must, or at least can, be done very differently. The fundamental sources of these differences are not well understood and subject to ongoing research.[4] As described later, a wide variety of differences in the background shape can be observed for pure elements (see, for example, the data collection of Moulder *et al.*[24]), and they can get increasingly for complex multi-element specimens with a variety of possible peak interferences and elemental distributions.

The shape of the background, mostly the slope of the background on the lower kinetic energy (higher binding energy) side of the photoelectron peaks, is also influenced by the distribution of the elements in the analysis volume; this is demonstrated by a useful example developed by Tougaard[7] and shown in Fig. 5. Tougaards' background models are theoretically based and model the distribution of electrons that lose energy due to inelastic scattering. The depth from which the electrons originate influences the number of electrons that lose energy due to inelastic scattering. Thus, the background produced by these electrons will vary depending on the depth distribution of elements being measured as highlighted in Fig. 5.

The variability in background shapes adds complications to the efforts to extract peak intensities above background and the nature of the backgrounds used when extracting information from peak fits. However, multiple approaches have been used quite successfully to reproducibly obtain useful information.

B. What is included in a photoemission peak?

Some photoelectron peaks are relatively simple, and separation of the background and peak appears to be intuitively clear. As noted by Brundle and Crist,[17] these occur for transitions, materials, and chemical states that have narrow symmetric peaks that have relatively low or "flat" backgrounds. However, other elements have photoelectron peak structures and are complicated by a variety of processes. In a discussion of terminology related to XPS, Baer and Shard[25] note that XPS peaks are influenced both by the initial state of the atoms prior to photoemission and final state effects that include multiplet splitting and shakeup and shakeoff processes that may both broaden peaks and introduce new peaks. Examples of the types of changes in spectral appearance are shown for copper in Fig. 6 where shakeup satellite peaks are introduced for CuO. Such peaks produced by final state effects contain electrons that are associated with the photoexcitation process and are appropriately part of the peak that should be included in Cu peak intensity for chemical quantification purposes. These are discussed in greater detail by Biesinger,[26] Thomas *et al.*,[27] and also in the perspective by Brundle and Crist.[17]

When collecting XPS data and either extracting the peak intensities by fitting these more complex spectra, it is necessary to

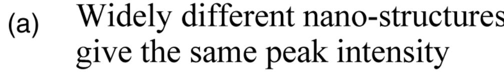

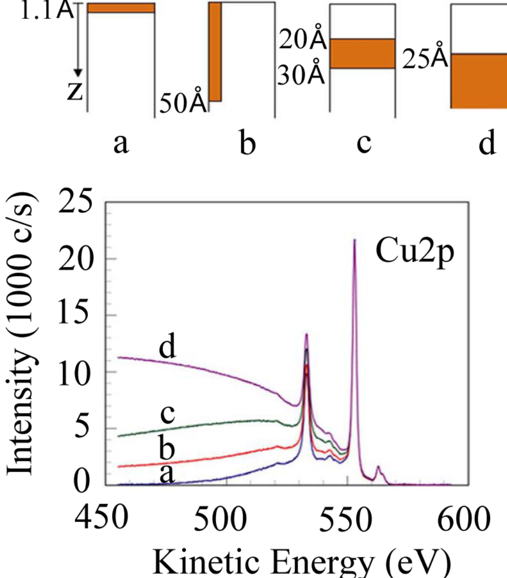

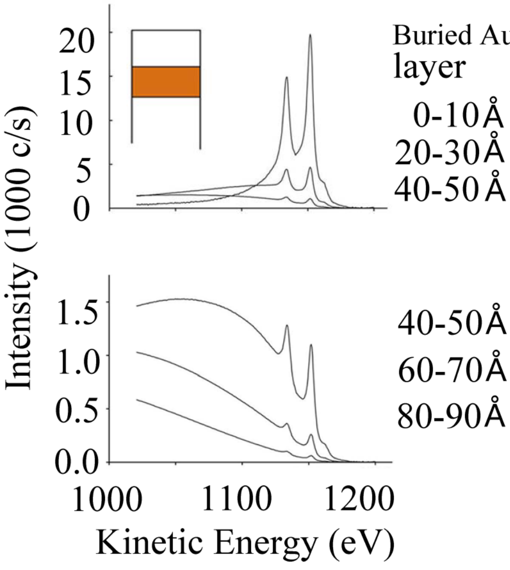

FIG. 5. Model XPS spectra for (a) Cu 2p for which the peak amplitudes are constant, but the background changes due to the Cu distribution and (b) Au 3d spectra for Au layers of different depths in a sample showing both changes in peak strength and background. Reprinted with permission from S. Tougaard, Surf. Interface Anal. **50**, 657 (2018). Copyright 2018 John Wiley & Sons, Ltd.

Downloaded from http://pubs.aip.org/avs/jva/article-pdf/doi/10.1116/6.0000359/15821876/063203_1_online.pdf

Published under license by AVS.

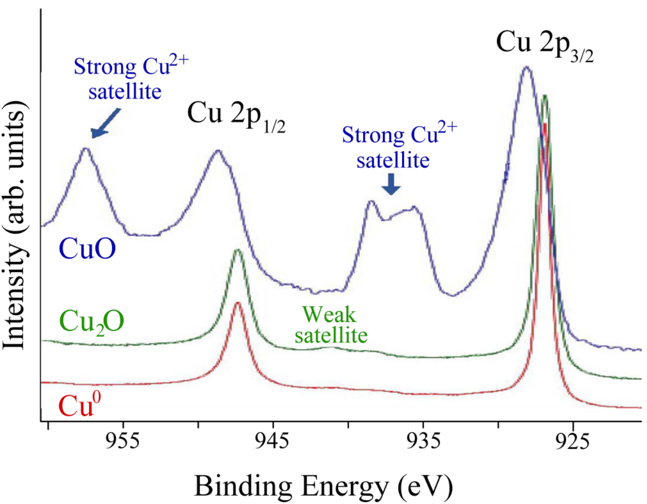

FIG. 6. Cu 2p spectra for a clean Cu metal surface, Cu_2O and CuO. Data provided by Thermo-Fisher. Note the particularly large satellite peaks for CuO.

recognize the importance of collecting data from an adequate energy range to include higher binding energy satellite peaks and to include the peak intensities in the data analysis. The analysts must be careful to select the entire spectral envelope when collecting the spectral data. Depending on the type of background subtraction method chosen for the analysis, the spectral region should extend well below and above the peak energy envelope. This will aid the analysts in selecting the end points required for background subtraction (see Sec. IV A 2). This is especially true when using the Tougaard[28,29] method of background subtraction since these background models involve inelastically scattered electrons that impact spectra to binding energies of 50–100 eV higher than the primary photoelectron peak. The analysts must also be careful that Wagner sensitivity factor data used for quantification, in general, do not include all satellite intensities. The analyst should include all peak intensities for best accuracy (See discussions in Sec. IV A 2 and Appendix A.).

III. BACKGROUND TYPES

A variety of backgrounds can be used to determine the peak area for quantitative analysis or for peak fitting to help with the chemical state analysis. A group of commonly used procedures have been developed to help the analysts in removing or subtracting the spectral background from the primary peaks of interest.[11,12] The most common background subtraction methods include linear,[30] original Shirley,[31] iterative Shirley,[10] and Tougaard.[29] However, as already noted, currently no theoretical model can fully reproduce the total background. Salvi and Castle[32,33] have shown that a combination of Tougaard and Shirley background can be used in the "active"[8] model for peak fitting. Some of the wide varieties of backgrounds that have been applied to XPS are shown in Table I. As can be seen, a few are in common use while others are less widely used or have become less used in time. Only more common background models are discussed below.

A. Linear background

A straight line[9,11–13,30] background shape is sometimes used to remove the background signal. A horizontal or sloped straight line is drawn between selected endpoints to form the background. A linear background may be satisfactory for spectra where there is no apparent step in the background over the energy range of the peak (e.g., the Cr 3s in Fig. 4). This method can be appropriate for a variety of s-type orbitals, where it is possible to align the background at both sides of the peak using a straight line. It was often used in the early days of XPS for a wider range of spectra and nowadays is not recommended for most spectra.

B. Shirley backgrounds

A Shirley[10–12,31] background in its original or iterative form is the most common method to deal with step changes in the background across the energy range of photoelectron peaks. This is an empirical method that assumes that the background at any chosen binding energy in the region of a photoelectron peak is proportional to the integrated intensity of the peak at higher

TABLE I. Overview of approach employed for background removal and fitting.

Background type	Mechanisms included	Use	Difficulty of use[a]	Reference
Linear	Empirical	Common	Low	30
Original Shirley (integral)	Empirical	Common	Low	31
Iterative Shirley	Empirical	Common	low	10
Shirley–Veigh–Salvi–Castle (SVSC)	Empirical	Uncommon	Low-moderate[b]	8, 33, and 34
Polynomial and exponential	Empirical	Uncommon	low	35
Tougaard—original	Inelastic scattering	Rare	High	29
Two and three-parameter Tougaard	Inelastic scattering	Common	Low	36
Five parameter Tougaard	Inelastic scattering	Rare	High	37
Partial intensity	Elastic and inelastic scattering	Rare	High	38
Combinations	Empirical	Increasing	Moderate	8, 14, and 39

[a]Some backgrounds are inherently simple to implement. Others commonly implemented in many data analysis systems are also easy to use.
[b]Can be easily implemented on a computer but not included in many data analysis systems.

Downloaded from http://pubs.aip.org/avs/jva/article-pdf/doi/10.1116/6.0000359/15821876/063203_1_online.pdf

Published under license by AVS.

kinetic energies. The background then involves a contribution that increases with the area under the photoelectron peak.

Figure 7 illustrates the situation using data from Pauly *et al.*[40] The analyst selects a start point (in this case a BE of 753.5 eV) and an end point (in this case, a BE of 696.4 eV). First, a linear flat background is removed from all the data points so that the point at a BE of 696.4 eV has zero counts. This removes the background shown as B1 in Fig. 7. In the Shirley method, the sum of the points from start to finish is calculated. This gives a total area of the spectral region above the background B1, which we can call A_T. The total area from a chosen point x to the end point is calculated, which we can call A_x. The Shirley background at each point x will be the difference in intensity at the start point minus the finish point times A_x/A_T. This gives the Shirley background B2. Since the difference in intensity at the start point and finish point is considerable in Fig. 7, it can be seen that both A_T and A_x will be in error because we want the areas to be calculated above the true Shirley background and not the background B1. Professor Shirley in his original paper[31] recognized this matter saying that "equation should in principle be iterated" but noted that it was not going to create a substantial error for the valence band spectrum of gold that was under study in his paper. One way of looking at this is that the background must meld smoothly into the experimental total signal, because if it does not, it would imply a sudden change in the shape of the background at the finish point that would be both arbitrary and physically unreasonable.

Proctor and Sherwood[10] reported an iterative approach where the process was iterated as a means of obtaining the correct background in the Shirley model rather than using the background B2. In the first step, a third iteration is conducted (where B1 is generated in the first iteration and B2 generated in the second iteration) by repeating the process using the background B2 rather than B1 to generate A_T and A_x. This process is continued in subsequent iterations until convergence is achieved. Convergence can be defined as occurring when the difference in A_T from one iteration to the next falls below a certain value. Typically, this value is 0.05 for the difference in the absolute value of (A_{Ti-1}/A_{Ti}) for the *i*th iteration. Usually, only a few iterations are needed, and in Fig. 7, convergence was achieved after six iterations, giving the iterative Shirley background B6. Below, we distinguish between four versions of Shirley backgrounds and terminology throughout this paper.

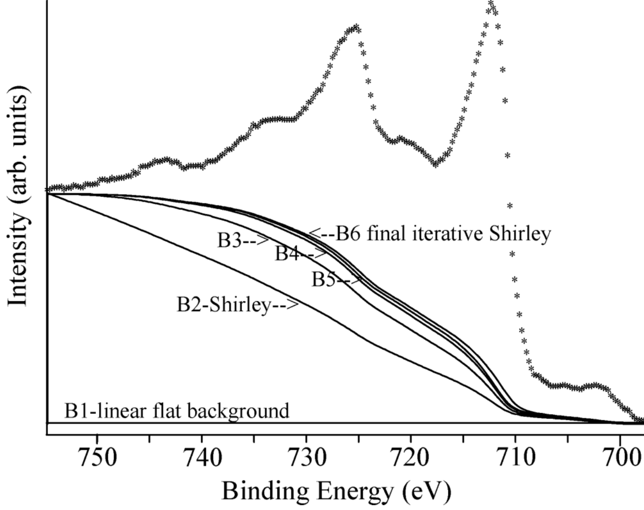

FIG. 7. Shirley and iterative Shirley backgrounds for the Fe 2p region of Fe_2O_3. Data taken from Pauly *et al.* (Ref. 40). The iterative Shirley background model uses Ref. 10.

1. Original Shirley (integral) background

As initially used by Shirley[31] for relatively simple valence band spectra, the background concept was applied without iterations. This simple, one pass, version of the Shirley background is also called the "integral background." It corresponds to B2 in Fig. 7.

2. Iterative Shirley background

The iterative Shirley background[10] is computed by performing the Shirley background routine successive times until convergence is reached using the criteria described above. Each iteration uses the previous iteration's background as its background as described above. The impact of iterations on the Shirley background is shown in Fig. 7. As noted above, when this background was first presented, it was recognized that the proper application of the background that Shirley described required iteration. We are calling the iterated form of the background the "iterative Shirley" background in order to provide a clear distinction from the original Shirley or integral background which is often simply (and correctly) identified as the Shirley background.

3. Smart background

The Smart background[41] is an iterative Shirley background to which a constraint has been added such that at no point will the background have a greater intensity than the actual data. Without this constraint, there are circumstances when fitting complex spectra for which the iterative Shirley background can apparently exceed the intensity of the measured spectra at that point.

4. Shirley–Vegh–Salvi–Castle background

This background, initially proposed by Vegh[34] and later on discussed by Castle and Salvi,[33] is based on a Shirley type background applied to a particular peak and not to the whole spectrum, as it is the case in the Shirley background. The details of its implementation are described elsewhere.[8] An example of a spectrum fit using this background can be found in Fig. 1 of Ref. 42.

C. Tougaard background models

The photoelectrons of higher kinetic energy that are inelastically scattered, so losing their energy, contribute to the background. A theoretical and computational approach calculating backgrounds due to extrinsic inelastic scattering was proposed by Tougaard and Sigmund in 1982.[29] This method is based on the electron energy loss function and uses an algorithm to generate the background due to inelastic losses. By considering any number of inelastic

Downloaded from http://pubs.aip.org/avs/jva/article-pdf/doi/10.1116/6.0000359/15821876/063203_1_online.pdf

Published under license by AVS.

events, it is shown that the background extends over a significant energy range. Herrera-Gomez *et al.*[4] comment that this approach is very successful for reproducing the background of 50 eV or so above the binding energy of the photoelectron peak but less successful at reproducing the types of background steps often observed nearer to the photoelectron peaks. Sherwood compared "active" peak fits with Tougaard and iterative Shirley backgrounds and found that the latter worked better for fitting peaks in a narrow energy range.[43]

1. Two and three-parameter Tougaard backgrounds

Rather than depending on obtaining the electron energy loss function for each material to be measured, Tougaard observed that depending on the class of materials, a function with either two or three parameters could be used to closely describe the differential inelastic cross sections (i.e., the electron energy loss function) of specific classes of materials.[36] For most metals, their oxides and alloys, a universal cross section for which there are two parameters is appropriate.[36,44] The two-parameter approach expresses the spectrum at energy E shown as $F(E)$ as being approximately equal to $j(E)$ (the measured spectrum after correction for the instrument transmission function) less the background expressed as a function containing the two parameters $\boldsymbol{B}$ and $\boldsymbol{C}$ and the electron energy loss $(E'-E)$ at energy E',

$$F(E) \approx j(E) - B\int_E^{\infty} dE' \frac{E' - E}{\left[C + (E' - E)^2\right]^2} j(E'). \tag{1}$$

Typical values for B and C are 2866 and 1643 eV^2. It should be pointed out, as clearly stated by Tougaard,[29] that this form of the background can only be applied to homogeneous materials. However, it is sometimes applied to thin layers by letting the B parameter to be included as part of a fitting process.

For most metals, their oxides and alloys, the universal cross section with two parameters has sufficient accuracy. For solids with a narrow plasmon structure, the cross sections cannot be well described by a function with two parameters. For these, however, it was found[36] that the main characteristics of the cross section can be described by the three-parameter universal cross section for which the parameters have been determined for several classes of materials (e.g., polymers, semiconductors, and free-electronlike solids).[40]

2. Slope background

The slope background can reproduce the change on the slope of the background signal before and after the peak region. It could be described as a one-parameter Tougaard background for the near-peak region.[45] However, its application can be extended to the cases in which the change on the slope cannot be reproduced through the Tougaard background [see Fig. 9(e)].

3. Modeling impact of elemental distribution on the background

As shown in Fig. 5, for inhomogeneous materials, significant different atomic concentration distributions (i.e., in-depth profiles) can result in identical photoinduced peak intensities but have significantly different backgrounds at binding energies above the photoelectron peak.[46] Formulae to determine the inelastic background for these inhomogeneous systems have been developed by Tougaard,[6] and they can be used to obtain the depth distribution of that element in the sample. The approach has also been used to examine coatings on nanoparticles.[47] A modeling program (QUASES) has been developed to use extracting depth information from experimental spectra[48] and an introductory guide to obtain depth information from back spectral backgrounds has been prepared as part of the XPS guide series.[49]

A number of other background approaches have been reported in the literature and described in ASTM and ISO guides.[11,12]

IV. CHOICES, CAUTIONS, AND COMMON ERRORS ON THE USE OF BACKGROUND MODELS

A. Choices in background selection and use

A user needs to make several choices in picking and applying a background model. Some of the advantages and limitations of the various background types were described above and will show up in examples later in the paper. Some choices may be limited based upon the software available and the speed for which the data analysis is needed. The background choice will also vary with the sample type and the type of analysis needed. The authors of this guide bring a set of differing approaches to the need and use of background models. One of the authors, M.H.E., is an "in the trenches" analyst working with a wide range of users at the U.S. Department of Energy user facility, often needing to extract information from spectra as quickly as possible. Sometimes this involves primarily extracting areas, while at other times peak fitting is required. P.M.A.S. has a long history in XPS including careful peak fitting and includes backgrounds as part of the fit.[9,43,50] A.H.-G. is involved in peak fitting but has a particular interest in understanding the fundamental nature of the background component in XPS spectra and has helped develop the active approach to background determination.[5] D.R.B. has used XPS to extract quantitative information related to environmental interactions involving metals, insulators, and nanoparticles. The importance of consistent quantification related to modeling in his research has led to a strong interest in testing and uniformizing, through appropriate standards and studies, the analysis practices within the applied surface science community. These varying interests and histories highlight some aspects of the different needs and approaches to address backgrounds in the XPS analysis.

Downloaded from http://pubs.aip.org/avs/jva/article-pdf/doi/10.1116/6.0000359/15821876/063203_1_online.pdf

1. Active or static

When analyzing data, there are two major ways that background models can be applied. The most common way to remove a background to obtain peak intensities is to identify the background, select relevant endpoints, and subtract the background from the measured spectrum: this is a "one shot" *static* approach. For some software packages, when a background is selected and applied, a new or altered spectrum with the background removed automatically appears in the region from which the area of the peak can be determined (or a fitting process initiated). From the perspective of fitting the data, this approach involves alteration of the experimental data with the subsequent curve fitting occurring on the altered

Published under license by AVS.

data, effectively constraining the fitting process by the endpoints of the spectrum and the background type selected by the analyst. Often such fits are displayed without the background present, but more recently, it has been possible to show the fit including the static background. As will be demonstrated in examples shown in Sec. IV B, the choice of background can alter the results of peak fitting, as well as peak intensity; if only the fitting of the altered data (without background) is displayed, it deprives a viewer of the ability to compare the original experimental data with the curve fit.

It is also possible for the background model to be included in the process of fitting a spectrum.[5,8,43] This active process involves inclusion of background parameters of the background model as variables in the curve fitting process. The *active* approach, described in more detail later, has specific advantages when doing curve fitting: (1) the analyst or other viewer can compare the original experimental data with the curve fit and the experimental data remain intact allowing the assessment of the overall quality of the curve fit and (2) allowing the fitting process to select the background parameters often improves the quality of a fit. It has been demonstrated that removing the artificial constraints imposed by the operator selected fixed starting and ending points allows for good quality fits to data for which the data collection range may be narrower than ideal.[8]

2. End point selection

In the guide to quantitative XPS analysis, Shard[18] comments that, for many spectra and some types of analysis, the selection of background end points can be as or more important than picking the background type. The dashed line shown in Fig. 8 will give significantly different peak intensities than any of the curves in the gray region. Two critically important issues to be considered: (i) how much of the spectrum is the photoelectron peak needed in the analysis (see Sec. II B and the discussion by Brundle and Crist)[17] and (ii) do the end points effectively average the background or have points that are effectively too low or too high been selected. Active fitting of the background can effectively mitigate both concerns: under that method, the intensity of the background in both sides is chosen transparently to the operator by employing the whole spectrum and not an average of a selected set of points, removing the need for the operator to choose the end points.[8,51] Since the background level might not coincide with any of the experimental end points, it is possible to fit too-short-range data for which the end points still have appreciable intensity from the peaks [see Fig. 1(d) from Ref. 8].

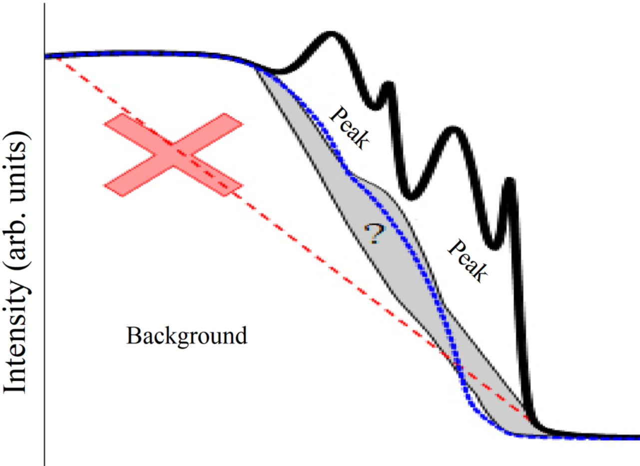

FIG. 8. Simulated XPS spectrum from the 2p region of a 3d metal with an oxide overlayer. The dashed line is an unreasonable linear background. Tougaard or Shirley backgrounds in the shaded area agree to the simulated model to within 10%. Figure 4 from Ref. 18. Reprinted with permission from A. G. Shard, J. Vac. Sci. Technol. A **31**, 041201 (2020). Copyright 2020, American Vacuum Society.

When active fitting is not employed, which is the case for most software, consistency of endpoint selection from the operator is important for quantitative analysis. Shard[18] also highlights the importance of reference materials for accurate quantitative analysis. The approach used to determine peak intensity for a reference material needs to be applied to the analysis of other related samples. The effect of the choice of the energy end points/regions on determination of the peak area has been discussed for the cases of the linear background[30] and the Shirley background.[10,14] Although often very useful, collections of sensitivity factors are not as accurate as the use of instrument developed sensitivity factors. Brundle and Crist[17] discuss differences between theoretically derived and experimentally determined sensitivity factors. The use of theoretically derived sensitivity factors requires the analyst to include all the relevant signals, including main peaks and other secondary peak features. The use of experimentally determined sensitivity factors requires that peak intensities be determined in a manner consistent with the way the sensitivity factors were obtained. In their background discussion, Castle and Salvi note that the empirical sensitivity factors developed by Wagner were frequently obtained using a Shirley background, though Wagner did establish some of his sensitivity factors from other authors who used straight line backgrounds.[33]

3. Nature of spectral background and model selection

Appropriate modeling of the background signal requires identifying regions of the spectrum in which the signal is pure background.[5,8] This requires that the energy range of the spectrum is wide enough to contain such regions (as described in the text regarding Fig. 1 of Ref. 8, this requirement can be relaxed if the active background approach is employed). Example spectra with different background features are shown in Fig. 9. The circled regions show regions of the “pure” background signal, while the dashed lines show the trends or nature of these backgrounds. Note that, for a sound fit of the data, the background needs to be considered in more detail than would be for simply extracting peak area. When parts of multiple photoelectron peaks overlap, the ability to clearly identify “pure” background regions of each element in the spectrum is more of a challenge. For one example, see the discussion in Appendix A.

Downloaded from http://pubs.aip.org/avs/jva/article-pdf/doi/10.1116/6.0000359/15821876/063203_1_online.pdf

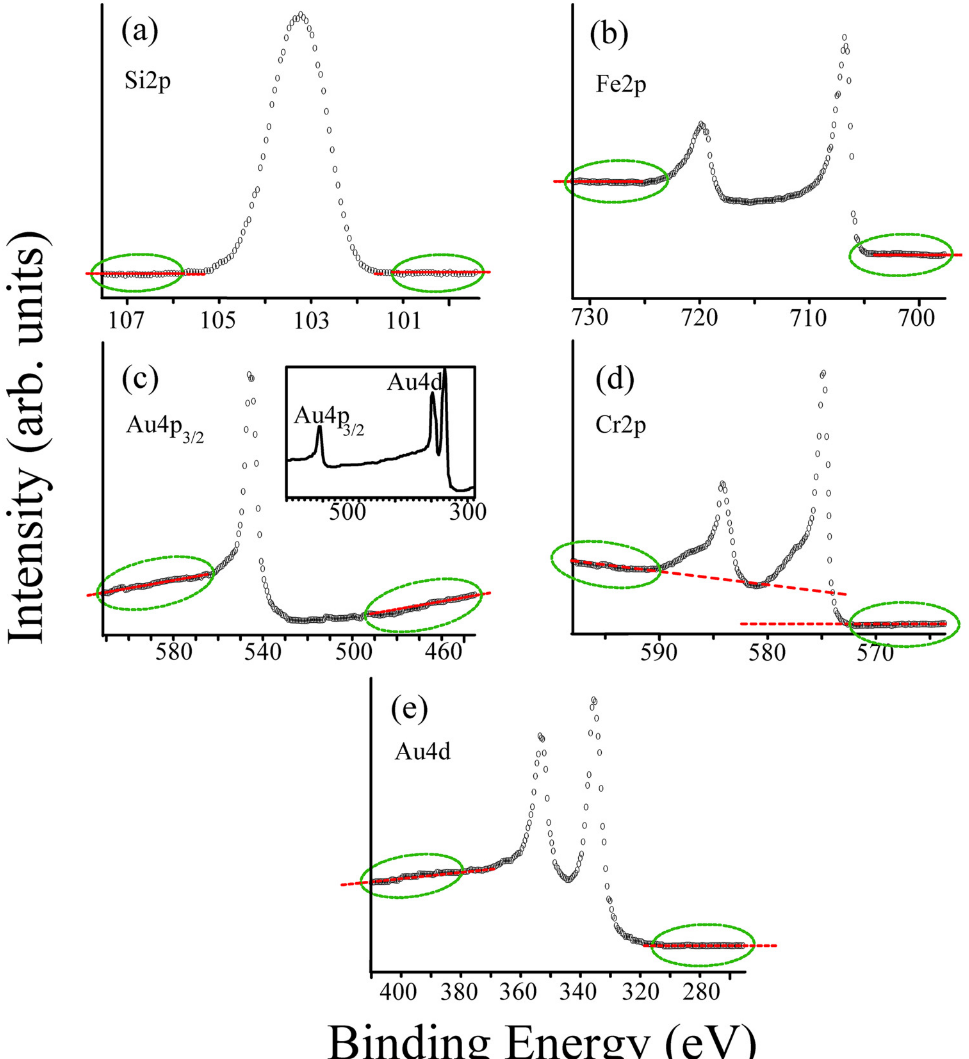

FIG. 9. Examples of spectra acquired with enough range to include regions of a pure background signal as indicated by the dashed ovals. The dashed lines (in red line) indicate the background trends. Strategies for background modeling of these spectra are discussed in the text.

Strategies for background fitting or subtraction are noted for each example. Note that in some cases it is useful to combine background models for the best data quality.

Figure 9(a)—The trend is very simple: it is the same for both sides and they can be joined by a simple straight flat line. In this case, the background is a simple horizontal line.

Figure 9(b)—There is a jump in the intensity of the background, but the slope is flat in both sides. The Shirley method can be employed to reproduce the step.

Figure 9(c)—There is a jump in the intensity and, in addition, the Au $4p_{3/2}$ peak lies on the decaying background signal of the Au $4d$ peak. This can be clearly observed in the inset. The background is then a combination of linear and Shirley backgrounds. Under the active background approach, which allows for the simultaneous use of various background types,[8] it is only necessary to select both types in software encompassing this approach (such as AAnalyzer[8,51]). The usual static way, although requiring additional effort for the operator/analyst, is to first remove the linear part[52] and then use the Shirley approach.

Figure 9(d)—Besides the jump, the slope of the background changes before and after the peak. In this case, it is necessary to simultaneously employ the Shirley method to reproduce the step and another method to reproduce the change on the slope. The two-parameter Tougaard background could be employed for the latter but without necessarily employing the exact theoretical value of the Tougaard B-parameter. The Shirley and Tougaard

Downloaded from http://pubs.aip.org/avs/jva/article-pdf/doi/10.1116/6.0000359/15821876/063203_1_online.pdf

Published under license by AVS.

backgrounds can be applied to the whole energy range under the active approach. The use of the active approach is highly desirable for fitting this type of spectra because it allows for the simultaneous optimization of both background contributions. If the active approach is not available in the software, it is possible to make an approximate determination of the peak area with a Shirley background applied to the near-peak region.

Figure 9(e)—Very similar to case (d), but the change on the slope is negative. It is still necessary to use a method to reproduce the jump and another to reproduce the change on the slope of the background from one side to the other. In this case, the Tougaard background cannot be used because it can only reproduce positive changes on the slope. The slope background can be used to reproduce negative slopes.[45]

These examples highlight some of the issues that an analyst might need to consider when analyzing peaks in the context of different general backgrounds. See also the discussion in the Appendixes A and B.

B. Static background removal impacts—Analysis of TiO_2 powder

When making measurements on real and often complex samples, an analyst must make a variety of choices including identifying the analysis objective, the nature and amount of data to be collected, the analysis approach, and the amount of time that can be devoted to each. Analysis can be complicated by ambiguity in the analysis needs, the form of the sample, the number of peaks present and peak overlaps, and the software readily available for analysis. In this section, the nature and impacts of some of these choices are explored while analyzing a TiO_2 anatase powder. The primary purpose of this example is to demonstrate the consequences of background selection on total peak area and relative intensity of spectrum components in relation to quantitative analysis. In addition, the example touches on other choices an analyst is required to make during analysis. This anatase example has been selected because it appears relatively simple but is complex enough that different background and analysis range choices have an impact on the results.

The sample material used in this example is a very lightly Pd doped (0.01 wt. %) TiO_2 anatase powder with particle sizes of approximately 13 nm as determined by XRD. The sample was pressed into a 3 mm diameter stainless steel sample stubs and pretreated *in situ* at 400 °C in 20% O_2/He at 100 sccm (standard cubic centimeters per minute) for 1 h (by *in situ* means in a vacuum chamber hard connected to the spectrometer). The *in situ* heating was performed in the effort to remove any residual surface contamination. The spectrometer used for collecting these data was a Physical Electronics (PHI) Quantera Scanning X-ray Microprobe. This system uses a focused monochromatic Al Kα X-ray (1486.6 eV) source for excitation and a spherical section analyzer. The x-ray beam is incident normal to the sample and the photoelectron detector is at 45° off normal. High-energy-resolution spectra were collected using a pass-energy of 69.0 eV with a step size of 0.125 eV. For the Ag $3d_{5/2}$ line, these conditions produced a FWHM of 0.92 eV ± 0.05 eV. The binding energy (BE) scale is calibrated using the Cu $2p_{3/2}$ feature at 932.62 ± 0.05 eV and Au $4f_{7/2}$ at 83.96 ± 0.05 eV. Because the sample demonstrated variable degrees of charging, the PHI charge compensation system was used, involving low energy electrons at ∼1 eV, 21 μA, and low energy Ar^+ ions ≈7 eV, to minimize this charging.

As suggested earlier, analysts are, to some degree, dependent on the software they are familiar with and have available for analyzing their data. The analysis shown in this section is an example of the approach that MHE would take using the PHI MultiPak[53] data analysis system on the Quantera scanning x-ray microprobe to process the data. Each instrument vendor provides analytical software with their system that can be used well by analysts experienced with them.

In almost all cases, it is important to collect XPS survey data from a sample to identify or confirm the overall composition, the presence of contamination and to help select regions of interest for more detailed analysis. The survey spectrum in Fig. 3 was collected before the higher energy-resolution data were collected. Although this sample was doped with a small amount of Pd, the only elements readily identified after the heating in the oxygen environment were Ti and O. It is also relevant to note that although the Ti 2p photoelectron peaks are near the O 1 s peak there is a nearly flat region between them that is useful to establish a useful background. However, the Ti 2 s peak contributes to a sloping background that will impact the high binding energy side of the O 1 s peak. In the discussion of the analysis below, attention is focused on high-energy resolution spectra of the Ti 2p region. Some discussions of the challenges in determining the O 1 s intensity are included in Appendix A.

These data were collected in the Environmental Molecular Sciences Laboratory (EMSL) Department of Energy User Facility. The user identifies the analysis needs and the initial analysis request for this sample was to determine if the Pd doping altered in a measurable way the electronic structure of the oxide nanoparticles. The sample was processed in oxygen to clean the sample and simulate a catalysts preparation step. High-energy-resolution spectra were collected for Ti 2p, O 1 s, and valence band regions. No effects of the dopants were identified. As it is often the case in EMSL, data collected for one purpose are sometimes asked to answer other questions. Here, we are exploring impacts of background type and endpoint selection on the relative intensity of the peaks observed in the Ti 2p spectrum and Ti to O ratio, which we expect to be Ti/O = 0.5. To allow others to try their own hand at analysis of the data discussed in this section, it has been submitted to *Surface Science Spectra*.[54] The peak areas shown in Tables II, III, and V allow other analysts to compare their measurements to those we obtained.

TABLE II. Ti 2p spectrum areas obtained after background subtraction and Ti/O ratios determined.

Background	Ti counts	O counts	Ti/O at. % ratio
Linear	374 510	157 864	0.77
Original Shirley	364 775	159 222	0.74
Iterative Shirley	268 258	157 583	0.55
Smart	268 402	157 864	0.55
Short iterative Shirley	203 906	157 583	0.42

Downloaded from http://pubs.aip.org/avs/jva/article-pdf/doi/10.1116/6.0000359/15821876/063203_1_online.pdf

Published under license by AVS.

TABLE III. Impact of different background subtraction models on apparent peak properties based on peak fitting. The percent Gaussian of the peaks was 80% in all cases.[a]

	2p3/2				2p1/2				Satellite loss 1			
Background[b]	BE	FWHM	Area	% Area	BE	FWHM	Area	% Area	BE	FWHM	Area	% Area
Linear	458.8	1.4	145 936	39.1	464	2.8	100 127	26.8	472	5.5	80 373	21.5
Shirley	458.7	1.3	154 270	42.7	464.4	2.7	90 829	25.2	472	5.6	72 180	20
Iterative Shirley	548.7	1.3	143 463	55.3	464.4	2.1	64 970	25.1	472.1	3.1	29 869	11.5
Smart	548.7	1.3	143 465	55.3	464.4	2.1	64 974	25.1	472.1	3.2	29 881	11.5

	Satellite loss 2				Satellite loss 3				Analysis	
Background	BE	FWHM	Area	% Area	BE	FWHM	Area	% Area	3/2 to 1/2 ratio	Total Ti counts
Linear	477.7	3.7	27 389	7.3	482.9	5.9	19 654	5.2	1.458	373 479
Shirley	477.8	3.6	25 319	7	482.8	6.2	18 567	5.1	1.698	361 165
Iterative Shirley	477.6	3.9	17 285	6.7	483.9	3.5	3 671	1.4	2.208	259 258
Smart	477.6	3.9	17 278	6.7	483.9	3.6	3 680	1.4	2.208	259 278

[a]In PHI MultiPak software, the 80% Gaussian means that the peak is a sum of 80% Gaussian shape and 20% Lorentzian shape.
[b]The endpoints for the linear background were 454–490 eV, while those for other backgrounds were 447–490 eV.

The same high-energy-resolution spectrum of the Ti 2p region of this oxide powder is shown in Fig. 10 with different backgrounds selected. Ti $2p_{3/2}$ and $2p_{1/2}$ spin orbit split peaks are shown along with what appear as three satellite loss features. As discussed in Sec. IV A 2, endpoint selection is an important choice that must be made by the analyst. Reasonable endpoint selections are shown for linear [Fig. 10(a)], original Shirley [Fig. 10(b)], and iterative Shirley [Fig. 10(c)] backgrounds.

Note how the iterative Shirley background melds smoothly into the experimental total signal, as noted above. A Smart background was also applied, but it was essentially identical to the iterative Shirley and therefore not shown. The endpoint selections in Fig. 10 are appropriate for the application of that background to the specific spectrum. Examples of inappropriate endpoint selections are shown in Fig. 11(a) for iterative Shirley backgrounds and in Fig. 11(b) for linear. The faulty background endpoints lead to not including all appropriate parts of the spectrum in Fig. 11(a) and the background crosses the spectrum in Fig. 11(b). Although these satellite loss features are theoretically predicted,[55] many of the Ti 2p spectra shown in the literature do not extend far enough to include the loss lines observed in this spectrum.[56,57]

The Ti 2p "altered" spectra after removal of the linear, original Shirley and iterative Shirley backgrounds are overlaid in Fig. 12 to highlight the differences due to the different choices of background removal. The spectra after linear and original Shirley are similar, but not quite identical, and are quite different than the spectrum after iterative Shirley (and Smart) background removal. There are two impacts of these differences: first, the peak intensities determined will differ and, second, the relative strengths of the components within the peak will differ. We first look at the impacts on peak intensity as summarized in Table II. The area attributed to the Ti 2p peak structure differs by roughly 40%. As would be expected from Fig. 12, the integrated Ti 2p intensities after linear and original Shirley background removal are similar, but not identical. The peak area after iterative Shirley and Smart background removal are essentially the same.

Quantitative analysis requires determination of the O 1 s signal intensity as well as that from the Ti 2p spectrum. This has its own set of choices that will be described in Appendix A. Based on one set of analyst choices (MHE), the O 1 s peak intensities (areas) using the same backgrounds are also shown in Table II. Note that these intensities do not show the same extent of variation as to the intensities extracted from the Ti 2p spectrum.

Also shown in Table II are Ti/O ratios obtained using the sensitivity factors of the PHI instrument on which the data are collected, which have been automatically adjusted for the specific measured transmission function of the instrument in the PHI MultiPak software. If the anatase sample is stoichiometric TiO_2, the Ti/O elemental ratio would be 0.5. The ratio of 0.55 suggests that the iterative Shirley and Smart backgrounds are more consistent with the instrument sensitivity factors than the other background removal methods. For comparison, the Ti 2p intensity obtained using the iterative Shirley background, but ignoring the loss lines, is included showing a significant impact on quantification.

It is important to note that the accuracy of XPS quantification when using the generic sensitivity factors is often stated as between 10% and 20% depending on the complexity of the sample, the complexity of the peaks involved, and the instrument set up. Thus, the 0.55 measured Ti/O ratio is not outside of what might be expected. Although it is important in most of the work in EMSL to find elemental concentrations that are "sensible," for many of the experiments desired information relates to changes in the relative concentrations and not absolute accuracy. For useful understanding of changes consistent background removal and analysis can provide the precision needed and absolute quantification is not required. Conrad *et al.*[23] point out that sometimes in software updates procedures may change. This highlights the value of maintaining graphs, end point information, and results of peak intensity that show the nature of the background removed in a particular data analysis for comparison with future analysis of similar data.

There are also unknowns and choices related to the determination of the O 1 s peak strength that impact some of the uncertainty

Downloaded from http://pubs.aip.org/avs/jva/article-pdf/doi/10.1116/6.0000359/15821876/063203_1_online.pdf

Published under license by AVS.

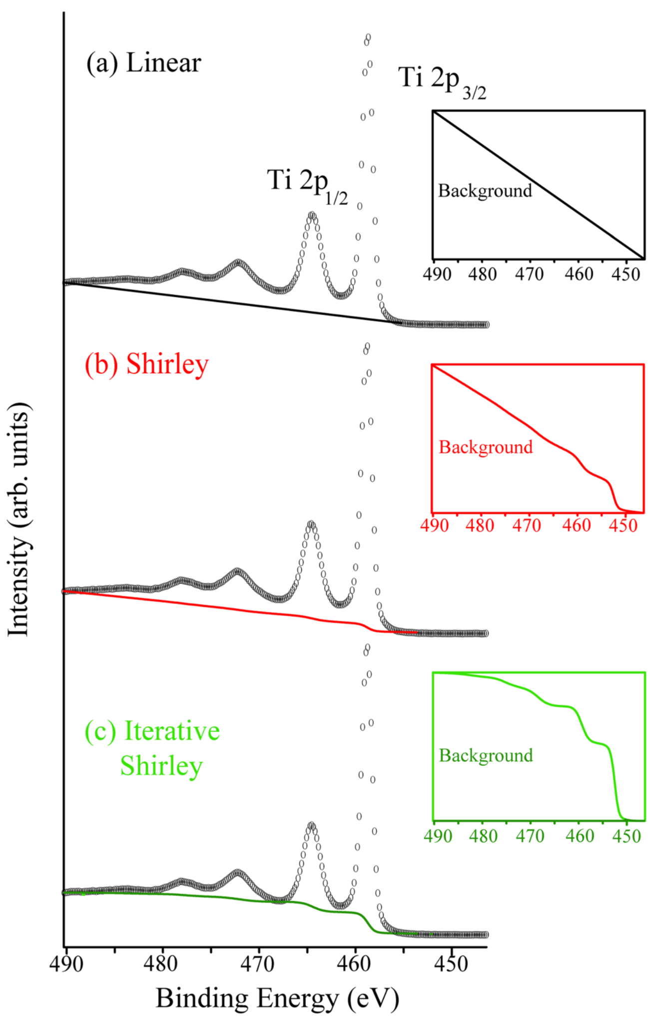

FIG. 10. Same Ti 2p spectrum with different backgrounds. The areas above the background are of interest for quantitative analysis. The areas determined after background removal are shown in Table II.

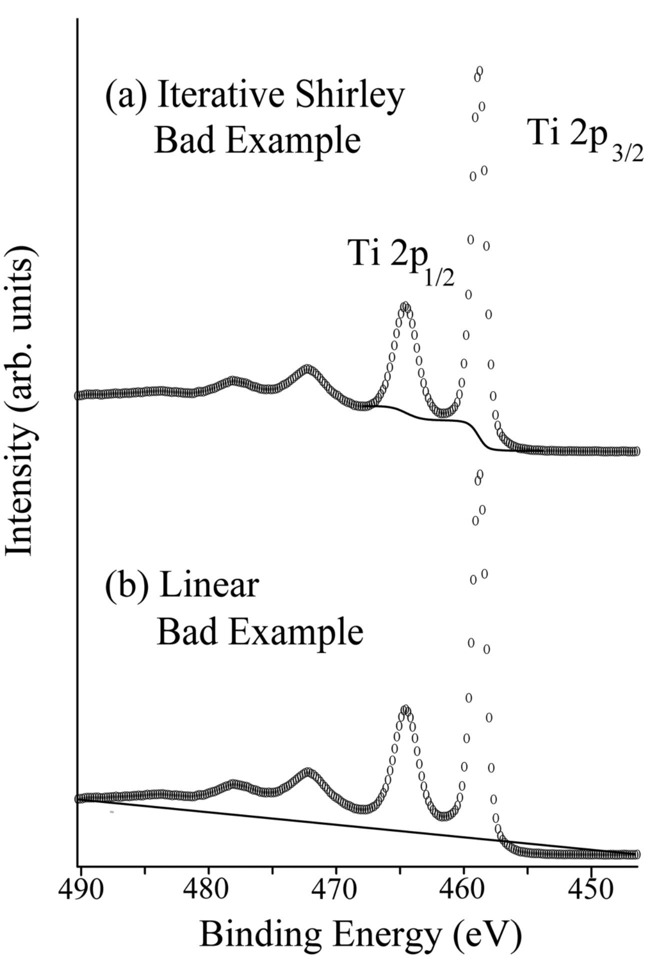

FIG. 11. Ti 2p same Ti 2p spectrum as in Fig. 8, with inappropriate background endpoints selected: (a) iterative Shirley that ignores loss peaks and (b) linear that intercepts the spectrum.

and these are briefly discussed in Appendix A and a little in Sec. IV C 1. It is also useful to remember that, with the use of reference materials on a well calibrated instrument and consistent well thought out measurement practices, XPS analysis can be both highly precise and highly accurate. The demonstrated impacts of differences in background removal highlight the importance of careful and consistent analysis.[18]

Backgrounds are critical to peak fitting as well as quantification. In the static mode, the altered spectra after background removal, such as shown in Fig. 12, are the spectra that are simulated by a curve fit. As demonstrated in the figure, the relative amplitudes of the Ti $2p_{3/2}$, Ti $2p_{1/2}$, and the satellite loss peaks are altered by the background selection. Such altered Ti spectra after removal of linear, integral, iterative Shirley and Smart backgrounds have been fit using the PHI MultiPak program with 80% Gaussian peak shape using a Gaussian/Lorentzian sum function. The results of this fit are shown after the iterative Shirley background removal. Figure 13(b) shows the fit to the background subtracted spectrum and Fig. 13(a) shows the fit with the background added back to the fit to show how the combination of background and fitting related to the initial experimental spectrum. Although many XPS data fits are shown only after background removal as in Fig. 13(b), it is much more useful to allow the reader to assess both the appropriateness of background removal and the quality of the fit to include the background as in Fig. 13(a).

The fitting of the four background subtracted spectra is summarized in Table III. The variations in peak width and relative amplitudes demonstrate the impact of background on the absolute and relative peak intensities obtained. The individual peak areas were summed to get a total Ti 2p intensity that is similar, but not identical, to that obtained from extracting the areas above

Downloaded from http://pubs.aip.org/avs/jva/article-pdf/doi/10.1116/6.0000359/15821876/063203_1_online.pdf

Published under license by AVS.

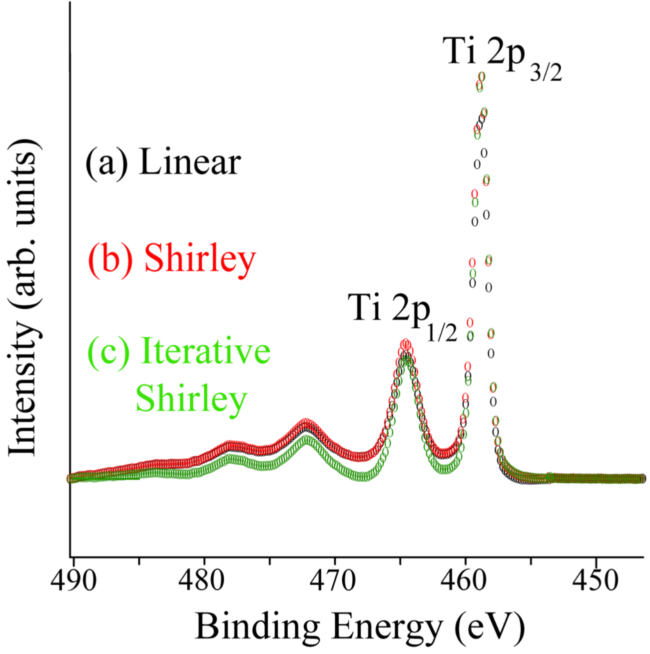

FIG. 12. Ti 2p spectrum after removal of linear, original Shirley, and iterative Shirley backgrounds. The overlay of these altered spectra highlights differences in the impacts of the background subtraction processes. Shirley and linear are similar but not identical as might be expected from the background shapes shown in Fig. 10.

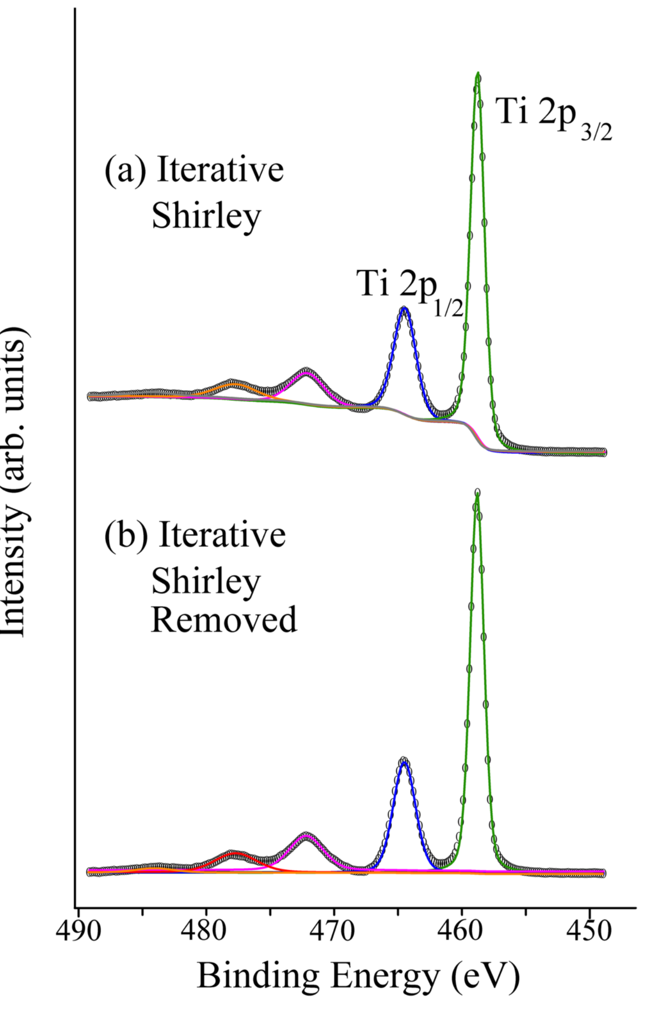

FIG. 13. (a) The Ti 2p spectrum shown previously simulated with a five peak fit as described in the text, shown with the background. (b) The fit in (a) shown without the background that was used. Plot (a) is the preferred display.

background as shown in Table II. In addition to the differences in the total Ti peak area, the peak fits show significant variations in the ratio of the $2p_{3/2}$ to $2p_{1/2}$ photoelectron peaks. Based on Scofield cross sections[58] this ratio should be 1.94, which is not true for any of these fits which were not constrained to this peak ratio. The iterative Shirley and Smart backgrounds over the whole range come closer than the linear or integral Shirley backgrounds. In discussing CasaXPS fits to Ti, Farley[13] notes that using an iterative Shirley fit for the $p_{3/2}$ and $p_{1/2}$ peaks individually produced the correct ratio. Using active background fits as described by Sherwood[9] and Herrera-Gomez[8] and discussed in Sec. IV C, it is possible to obtain peak fits fully consistent with the physical and chemical nature of the material. In this example, we see that for quantitative analysis of the relative amounts of Ti and O present in the sample, the iterative Shirley and Smart backgrounds appear to work satisfactory, likely because the sensitivity factors were determined in a similar manner in how they included the shake satellite intensities. However, the physical and chemical details of the fits to the spectrum are not fully correct.

It is likely that most of the quantitative analysis and peak fitting reported in the literature has been done using static background removal. When carefully and consistently done it can provide the needed information. As of May 2020, the Wiki description of peak fitting suggests that the process of peak-fitting high-energy resolution XPS spectra is still a mixture of art, science, knowledge, and experience. That same statement applies to dealing with static background removal. The active fitting process and background removal described in Sec. IV C does not depend on operator selected endpoints and by intent and practice decreases some of the sensitivity to operator selections.

C. Comparison of active versus static background for fitting—TiO_2 and oxidized W

In the "active" approach, the background is included in the curve fitting process and not dependent upon user selected endpoints as described above. If the background removal in the "static" approach were perfect, the two approaches would be equivalent. Unfortunately, there is no "perfect" background removal process. Particularly for studies requiring curve fitting, the selection of

Downloaded from http://pubs.aip.org/avs/jva/article-pdf/doi/10.1116/6.0000359/15821876/063203_1_online.pdf

Published under license by AVS.

background parameters, such as background type and beginning and ending points, can have a significant impact on the results.

The active approach to backgrounds has specific advantages[8,43] that will be highlighted in the examples to follow, some of which are indicated in method comparison in Table IV. However, the implementation of active background processes requires appropriate software that is not included in many instrumental based analysis systems.

1. Anatase TiO_2 revisited

As a first example of the application of an active background, we look again at the anatase spectrum that was examined in a static mode in Sec. IV B. The simple fits shown in that section demonstrated impacts of background on relative peak strength and total peak intensity. However, as noted in the analysis section of Table III, the fits after background removal did not appropriately reflect all of the relevant physical and chemical characteristics of the spectrum. Even for this relatively simple spectrum, a chemically meaningful fit should include a correct representation of the known physical and chemical characteristics of the sample and the photoelectron process potentially including meaningful peak widths, peak ratios, and correct stoichiometries. TiO_2 is a material where there are significant effects leading to the Ti $2p_{1/2}$ peak being significantly broader than the Ti $2p_{3/2}$ peak. Recently,[59] the attribution of this difference in width to super Coster-Kronig effects has been challenged and the broadening of the Ti $2p_{1/2}$ peak has been attributed to the presence of XPS intensity distributed over many unresolved final states for a Ti $2p_{1/2}$ peak core hole. While we fit these Ti 2p peaks to two peaks, the recent work suggests that there may be additional intensity between the two peaks. In careful fitting of such spectra it is important to ensure that the relative areas of the two spin–orbit split peaks have the correct area ratio while allowing the FWHM of the two peaks to differ. Such effects are discussed in the fitting perspective by Sherwood.[9]

TABLE IV. Comparison of active and static backgrounds.

Static	Active
Linear, Shirley, and possibly Tougaard algorithms available in most data analysis systems	Requires fitting program that includes background and peak parameters, not available on most instrument-based data analysis systems
User picks background type and endpoint selection forces background to pass through user selected points that do not change. Constrains peak shapes during fit	User picks background type(s), fitting adjusts background parameters, usually resulting in higher quality fit
Need good background trend information (e.g., Fig. 9) to use background removal without impacting area or fitting options	Fitting the background can make up for restricted data range and has less impact on determining peak widths and areas
Linear, Shirley, and other backgrounds may be removed sequentially	Fitting gives appropriate combination if more than one background type is needed
The effect of uncertainty on the background on the peak parameters must be added afterward using methods developed *ad hoc* for this purpose	The uncertainty on the fitting parameters, including the covariances with the background parameters, can be calculated through the covariance matrix

As example of an active fit to the TiO_2 spectrum discussed above using the active approach is shown in Fig. 14. The fitting process included linear slope and Shirley Vegh Salvi Castle (SVSC) backgrounds, maintained the $2p_{3/2}$ to $2p_{1/2}$ ratio at 1.94 and included pairs of two satellite peaks associated with the $2p_{3/2}$ and $2p_{1/2}$ photoelectron peaks at the same 1.94 ratio. The results from this fit are shown in Table V and compared to static fits from the same program.

The nature of the fitting conducted by the AAanalyzer program has significant differences in comparison to those conducted using the MultiPak program reported above including enabling two background types to be used in peak fitting during the active peak fit (not forcing the background to pass through two user selected points), restraining the $2p_{3/2}$ to $2p_{1/2}$ peak ratios to the physically correct values, and using the appropriate Voigt peak shape for the fits.[9,51] Note that the total Ti 2p area obtained using the *iterative* Shirley background was essentially the same as reported in Table III and this area is somewhat smaller than that obtained using the active fit, consistent with earlier reports.[8] The Ti/O atomic percent ratios were obtained using the same sensitivity factors used in Table II and the results are slightly closer to the

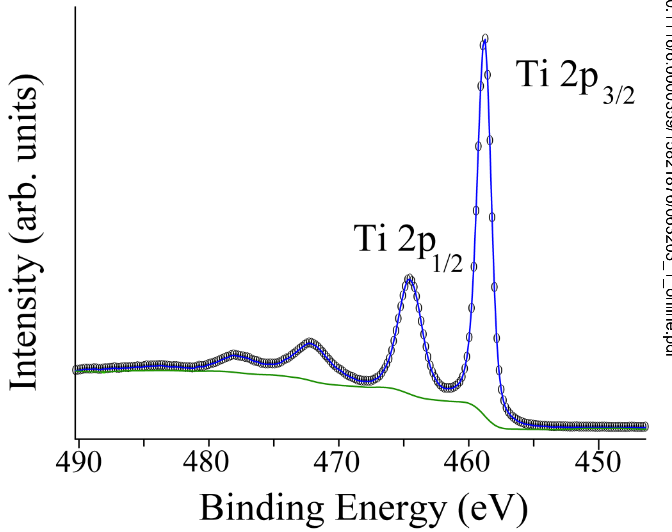

FIG. 14. Ti 2p spectrum from anatase including an active fit to peaks and background. The backgrounds included in the fit were the Shirley type SVSC and a linear background. This active fit using the AAnalyzer program maintains the proper $2p_{3/2}$ to $2p_{1/2}$ ratio of 1.94 and maintains a similar appropriate ratio for pairs of the satellite loss peaks.

Downloaded from http://pubs.aip.org/avs/jva/article-pdf/doi/10.1116/6.0000359/15821876/063203_1_online.pdf

Published under license by AVS.

TABLE V. Peak fitting parameters from AAnalyzer active fit and static original and iterative Shirley fits. Compare results to previous static fit parameters in Table III.

Background	$2p_{3/2}$				$2p_{1/2}$				Sat1 $2p_{3/2}$			
	BE	FWHM (V)[a]	Area	% Area	BE	FWHM (V)[a]	Area	% Area	BE	FWHM (G)	Area	% Area
Active	458.7	1.24	145 236	53.0	464.4	2.13	74 864	27.3	471.9	3.38	31 706	11.6
Static original Shirley	458.7	1.25	154 402	51.0	464.4	2.27	79 588	26.3	472	4.24	45 376	15.0
Static iterative Shirley	458.7	1.24	140 518	52.4	464.4	2.08	72 432	27.0	472.1	3.43	31 808	11.9

Background	Sat1 $2p_{1/2}$				Sat2 $2p_{3/2}$				Sat2 $2p_{1/2}$			
	BE	FWHM (G)	Area	% Area	BE	FWHM (G)	Area	% Area	BE	FWHM (G)	Area	% Area
Active	477.5	3.84	16 343	6.0	484.2	3.38	4 046	1.5	490	3.38	2 085	0.8
Static original Shirley	477.7	4.18	23 389	7.7	484.2	4.24	0	0.0	490	4.24	0	0.0
Static iterative Shirley	477.6	3.53	16 396	6.1	483.4	3.43	4 701	1.8	498.1	3.43	2 423	0.9

Background	Analysis			
	Total 2p	$P_{3/2}$ to $P_{1/2}$ ratio	O 1s	Ti/O at% ratio
Active	274 280	1.94	166 712	0.53
Static original Shirley	302 755	1.94	169 095	0.58
Static iterative Shirley	268 278	1.94	168 389	0.51

[a]The peaks were fit with Voigt functions by the AAnalyzer program and the fit of the 2p photopeak reported both Gaussian (G) and Lorentzian (L) FWHM information. The satellite peaks returned only Gaussian peak widths. The combination of G and L FWHM information was turned into an approximate Voigt FWHM using equation FWHM (V) = 0.5346 * FWHM(L) + (0.2166 * FWHM(L) + FWHM(G))$^{1/2}$ from Olivera and Longbothum.[60]

expected value of 0.5 for the active and iterative Shirley backgrounds reflecting a difference in the O 1 s intensities discussed in Appendix A.

In many ways, the results from the active fit are like those from the static background removal reported in Table III, except that the proper physical intensity ratios are maintained, and other physics of the expected signals are produced. The next example will highlight conditions for which the active background approach will be of increased importance.

2. *Impacts of background selection on fitting of complex spectra—Oxidized W example*

The anatase example identified some of the issues associated with background removal from the relatively simple single component spectrum. Complexity can be introduced to spectra in multiple ways including photoelectron peaks introduced by x-ray satellites from achromatic (i.e., nonmonochromatized) x-ray radiation sources (discussed in Appendix B), inherently complex structures of the photoelectron peak of interest, peak interferences due to elements with overlapping or adjacent photoelectron peaks, and the presence of two or more chemical states including the photoelectron elemental spectrum. Each of these can complicate determining the appropriate background of the photoelectron peaks of interest impacting quantitative analysis and fitting of peaks. Figures 15–17 show different data analysis approaches to a spectrum of an oxidized W example that includes the presence of multiple chemical states in a spectrum obtained using an achromatic x-ray source. The discussion here focuses on background effects during curve fitting, not primarily on the fitting process which is discussed in more detail elsewhere.[9,10,13,19,50]

In Figs. 15 and 16, we compare the behavior of the calculated background using the "active" and the "static" approaches and show how the chemical information obtained for the oxidized W example varies substantially depending upon the background and curve fitting approaches that are used. The iterative Shirley method will be used for all the backgrounds in this comparison.

One might start with the proposition that there should be no difference between the "active" and "static" approaches if the removal of the background from the experimental spectrum were "perfect" when using the "static" approach. This proposition can be tested by the example in Fig. 15. This figure shows an "active" [Fig. 15(a)] and a "static" approach [Fig. 15(b)], together with a "static" approach with a background correction by using a sloping linear background [Fig. 15(c)]. If the initial background subtractions were "perfect," then Figs. 15(a) and 15(b) should be identical, which they are clearly not. Table VI shows how the different approaches impact both the total fitted area of the region studied as well as the relative amounts of the fitted components and the quality of the fit. In all three cases in Fig. 15, we have used a Gaussian–Lorentzian product function[61] with the same peak shapes for the various tungsten species. The curve fitting process gave the same peak widths for Figs 15(a) and 15(c), and slightly less (by less than 0.1 eV) for Fig. 15(b). It is clear from Table VI that Fig. 15(b) is a much poorer fit (with a much larger reduced χ^2 value) than Figs. 15(a) and 15(c), with Fig. 15(a) being the best fit. The use of a sloping linear background in Fig. 15(c) improves the

Downloaded from http://pubs.aip.org/avs/jva/article-pdf/doi/10.1116/6.0000359/15821876/063203_1_online.pdf

Published under license by AVS.

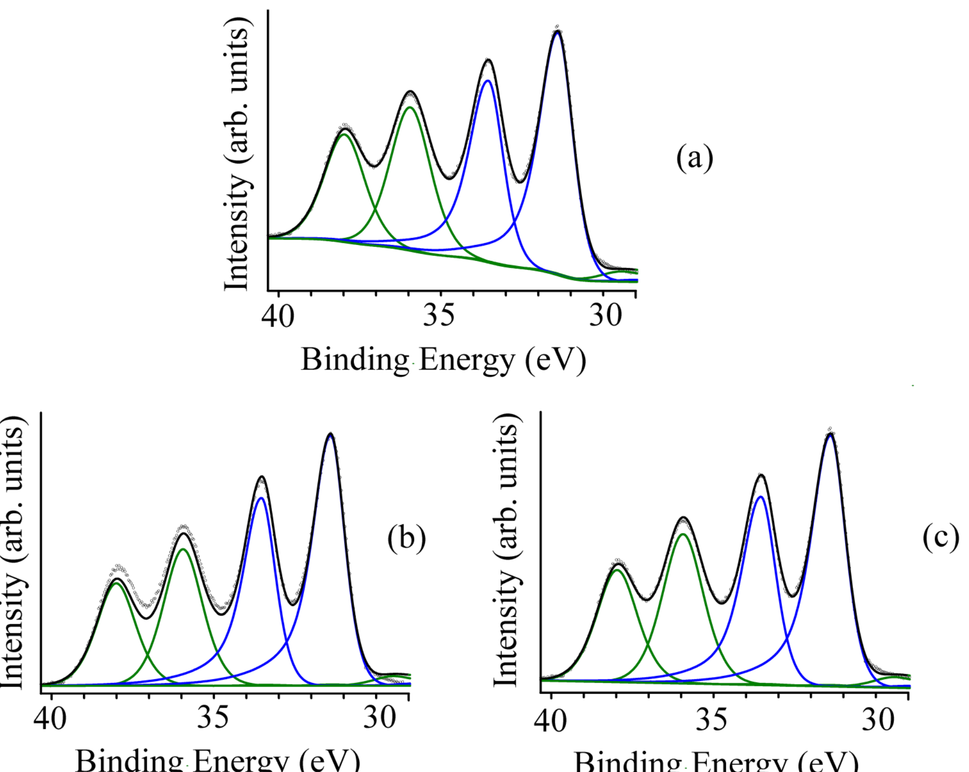

FIG. 15. W 4f spectrum of metallic tungsten with a surface oxidized layer obtained with MgKα achromatic X-radiation fitted to spin–orbit split peaks for the metal and oxidized tungsten using different background models and Gaussian/Lorentzian product functions with an exponential tail (Ref. 61). Data taken from Ref. 10 (a) shows an "active" curve fit with an iterative Shirley background included in the fit. (b) shows a "static" curve fit to the original spectrum after removal of an iterative Shirley background and then fitted with a horizontal linear background included in the fit. (c) shows the original spectrum after removal of an iterative Shirley background and then fitted with a linear sloping background included in the fit. Note that satellite x-ray peaks appear at low BE due to the achromatic source causing an offset that needs to be considered during static background selection. Peak information is contained in Table VI.

fit by adding an additional background correction showing that the background was not correctly assessed in the background subraction of the original data. This reflects the fact that the "static" approach, which requires the user to select the correct background parameters, did not correctly account for the background. Note how the total fitted area in Fig. 15(b) is significantly less than in Figs. 15(a) and 15(c). The initial choice of background parameters has not correctly accounted for the x-ray satellite features that arise from the W4f oxidized tungsten peaks, leading to the poor fit in Fig. 15(b). X-ray satellite features are discussed in Appendix B.

This example illustrates the benefit of using the "active" approach by including the background in the fit. The "active" approach also retains the unaltered experimental data allowing a proper assessment of the chosen data analysis. Figure 15(a), while a good fit to the original experimental data is, like all curve fitted data, not a unique fit. The analyst needs to consider not only the choice of background model to be used in the "active" approach, but also the fitting function and the number and types of component peaks to be included in the fit. These component peaks might include chemically shifted oxidized features, satellite features, and x-ray satellite features when achromatic radiation is used.

Appendix B gives more details of how these considerations impact the information provided by an analysis of the spectrum. Appendix B addresses the following:

- There is a low intensity W 5p peak from the metal that should be included in the fit.
- The fit needs to include another oxidized tungsten species identified as W(V)? in Table VI.
- It is appropriate to use a more scientifically correct Voigt function and a function for the metal which has more Lorentzian character.
- The choice of the background model in the "active" approach impacts the total fitted area and the relative amounts of the different tungsten species.

Figure 16 and Table VI show the appearance of the spectrum when an "active" fit is carried out with additional tunsten features, more metal Lorentzian character, and a Voigt function. Figure 17 and Table VI show the appearance of the spectrum when an "active" fit is carried out as in Fig. 16(b) (Voigt function used) with different background models. The widths of the peaks fitted in Fig. 17 are nearly identical for all three background models. The total fitted

Downloaded from http://pubs.aip.org/avs/jva/article-pdf/doi/10.1116/6.0000359/15821876/063203_1_online.pdf

Published under license by AVS.

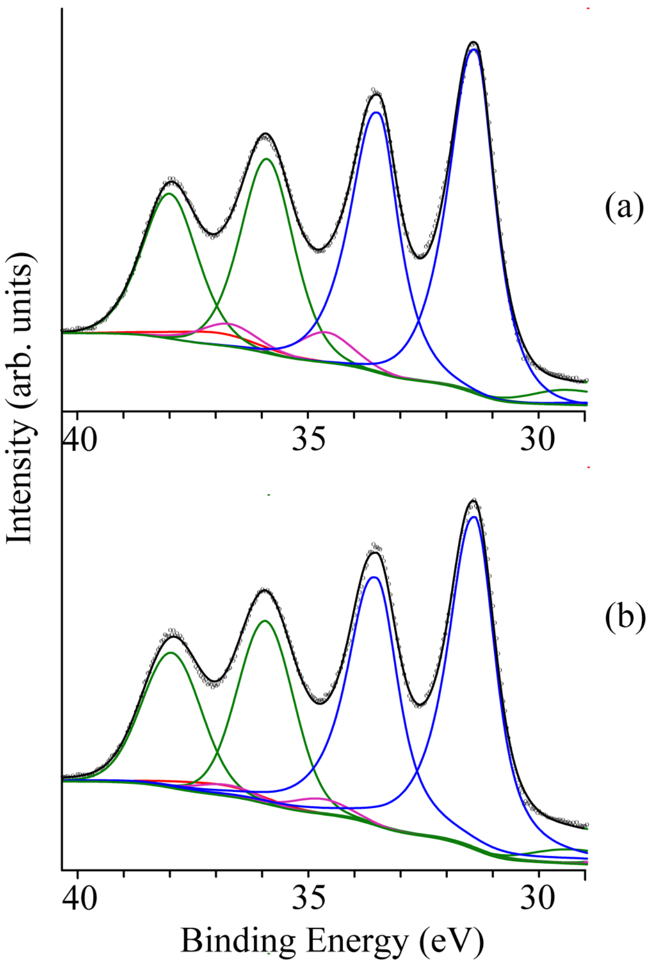

FIG. 16. Data in Fig. 15 fitted in (a) to Gaussian/Lorentzian product functions and in (b) to true Voigt functions. An iterative Shirley background and a W 5p peak missing in Fig. 15 were included in both fits. Peak information is contained in Table VI.

area increases in the order iterative Shirley < linear sloping < Tougaard. This illustrates how quantitation calculations, which depend upon the area of the fitted peak, are impacted by the choice of background model.

D. Background removal for valence band spectra

The valence band XPS spectral region contains a considerable amount of chemical information and is complementary to the information provided by the core XPS region, often being able to distinguish subtle chemical differences that cannot be obtained by a study of the core region.[62] This region cannot be analyzed by curve fitting because the spectral appearance is dominated by chemical bonding effects complicated by the dispersion of energy levels for different directions in the solid. Valence band spectra can be analyzed by comparison with calculated spectra often obtained from band structure calculations. In making these comparisons, it is helpful to remove a background. The initial presentation of the Shirley background removal was assocaited with valence band spectra.[31]

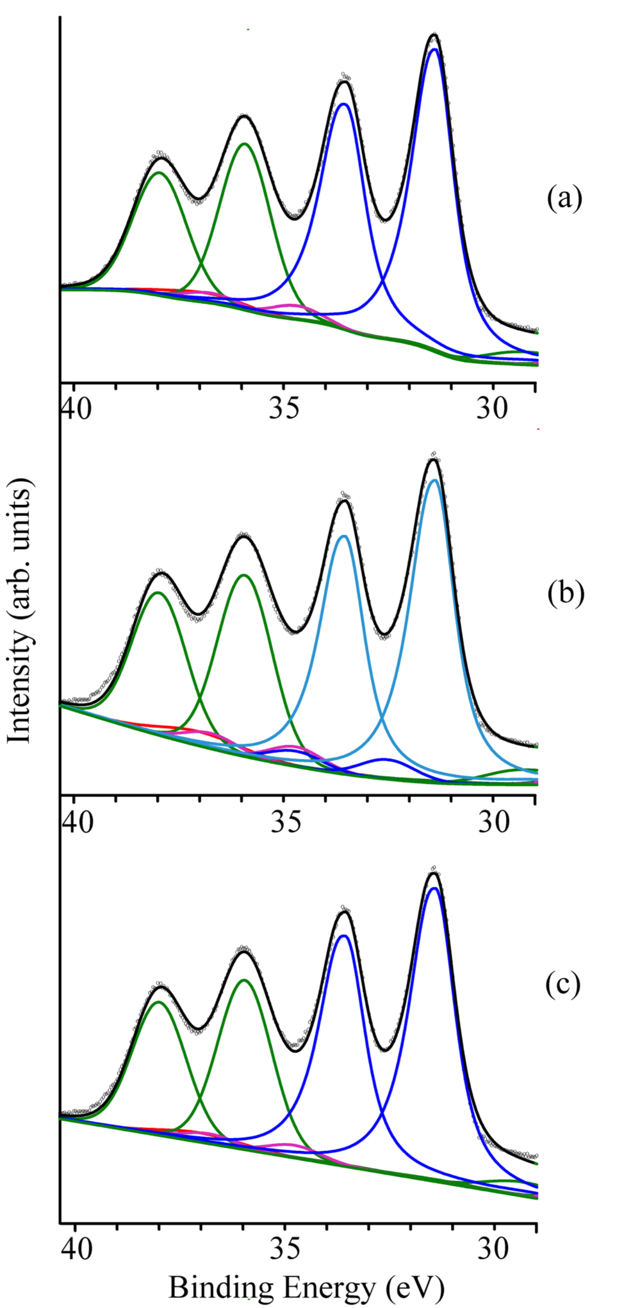

FIG. 17. Data in Fig. 13 fitted to true Voigt functions and application with different background models: (a) An iterative Shirley background, (b) a Tougaard background, and (c) a linear sloping background.

Downloaded from http://pubs.aip.org/avs/jva/article-pdf/doi/10.1116/6.0000359/15821876/063203_1_online.pdf

Published under license by AVS.

TABLE VI. Influence of background choice and background approaches in curve fitting oxidized tungsten.

Background	Active mode	Species	Peak	Area as % total area	Reduced χ^2	Total fitted area (cts/eV)
Iterative Shirley	Yes	Metal	$W4f_{7/2}$	35.19	10.45	245 162
background included in the fit			$W4f_{5/2}$	26.39		
[Fig. 15(a)]		WO_3	$W4f_{7/2}$	21.96		
			$W4f_{5/2}$	16.47		
Iterative Shirley	No	Metal	$W4f_{7/2}$	36.35	670.35	227 141
background removed then fitted with a			$W4f_{5/2}$	27.26		
horizontal background included in the fit		WO_3	$W4f_{7/2}$	20.79		
[Fig. 15(b)]			$W4f_{7/2}$	15.59		
Iterative Shirley	No	Metal	$W4f_{7/2}$	35.14	14.29	246 215
background removed then fitted with a linear			$W4f_{5/2}$	26.39		
sloping background included in the fit		WO_3	$W4f_{7/2}$	22.00		
[Fig. 15(c)]			$W4f_{5/2}$	16.47		
Iterative Shirley background included in the	Yes	Metal	$W4f_{7/2}$	32.48	11.84	247 178
fit with Gaussian/Lorentzian product			$W4f_{5/2}$	25.53		
functions and correct metal tail			W5p	1.91		
[Fig. 16(a)]		WO_3	$W4f_{7/2}$	19.39		
			$W4f_{5/2}$	15.21		
		W(V)?	$W4f_{7/2}$	3.07		
			$W4f_{5/2}$	2.41		
Iterative Shirley background included in the	Yes	Metal	$W4f_{7/2}$	35.33	15.68	270 546
fit with true Voigt functions and correct			$W4f_{5/2}$	27.74		
metal tail			W5p	1.75		
[Figs. 16(b) and 17(a)]		WO_3	$W4f_{7/2}$	18.20		
			$W4f_{5/2}$	14.26		
		W(V)?	$W4f_{7/2}$	1.52		
			$W4f_{5/2}$	1.19		
Tougaard background included in the fit with	Yes	Metal	$W4f_{7/2}$	32.16	26.95	314 655
true Voigt functions and correct metal tail			$W4f_{5/2}$	25.28		
[Fig. 17(b)]			W5p	2.24		
		WO_3	$W4f_{7/2}$	18.57		
			$W4f_{5/2}$	14.59		
		W(V)?	$W4f_{7/2}$	1.99		
			$W4f_{5/2}$	1.57		
		WO_2	$W4f_{7/2}$	2.01		
			$W4f_{5/2}$	1.58		
Linear sloping background included in the fit	Yes	Metal	$W4f_{7/2}$	34.75	35.75	287 972
with true Voigt functions and correct metal			$W4f_{5/2}$	27.31		
tail			W5p	1.61		
[Fig. 17(c)]		WO_3	$W4f_{7/2}$	18.92		
			$W4f_{5/2}$	14.88		
		W(V)?	$W4f_{7/2}$	1.42		
			$W4f_{5/2}$	1.11		

Figure 18 illustrates this approach for the valence band of metallic molybdenum,[63] which has a complex spectrum and considerable dispersion with the experimental spectrum shown with the removal of a background using the Tougaard approach and the iterative Shirley approach for comparision with a calculated spectrum.[62,63]

E. Software options

Computer software provided with most XPS instruments has powerful data analysis techniques, including background removal and curve fitting functions. The PHI instrumental package MultiPak was used for the analysis reported in Sec. IV B. Other

Downloaded from http://pubs.aip.org/avs/jva/article-pdf/doi/10.1116/6.0000359/15821876/063203_1_online.pdf

Published under license by AVS.

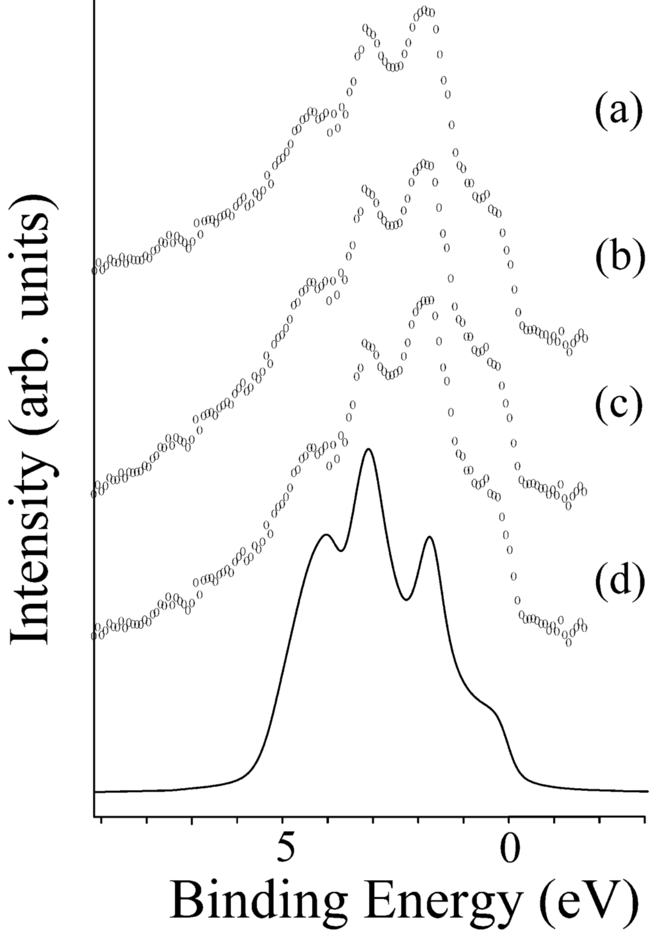

FIG. 18. XPS valence band spectrum of metallic molybdenum obtained with monochromatic AlKα X-radiation with the original spectrum (Ref. 63) in (a), the spectrum with a Tougaard background removed in (b), the spectrum with an iterative Shirley background removed in (c), and the calculated spectrum in (d).

software packages are available both as commercially developed and from individual researchers. The widely used commercial package is CASA XPS[13] which provides a wide range of capabilities and options. The program applied in Sec. IV C 1 was AAnalyzer described and used by AH-G[8,51] for active fitting of data. PMAS uses his own software which was developed over many years from the 1970s to the present, originally developed at a time when there was very little commercial software available, the software being used for routine data analysis and for developing data analysis techniques. This software has been made available to a number of research groups.[9,43,50] The authors listing and uses of these software packages are provided by example with the hope that the information will be useful for any software packages that are available to an analyst.

V. WHAT IS CORRECT OR GOOD ENOUGH?

The "active" approaches discussed above clearly gave the best fit in terms of the appearance of the fit and the lowest χ^2 value (Appendix B). It is important to ask whether results from any background removel or any fit, including peaks and background, make good scientific sense and provide useful information. A variety of approaches and criteria can be used to assess in different ways the appropriateness and quality of the background removal approaches that have been applied, some depend on the application or purpose of the analysis. It is relevant to remember that aspects of the backgrounds in XPS spectra are not fully understood so that there is no totally correct approach available at this time, but there are appropraite ways to assess the approaches used.

- Is the background approach that has been used adequately described and/or displayed? Without adequate information, it is not possible for others to assess in any way the appropriateness or quality of what has been done.
  - Reports and journal articles should have adequate information for others to understand and repeat the analysis. ISO technical report 18392 provides relevant background and ISO standard 19830 indicates reporting requirements for peak fitting, which include reporting of spectra background parameters.
  - The background used to model or fit data should be displayed.
- A first order check on appropriateness is a visual check of the background relative to the spectrum.
  - How well does the background relate to the spectrum? Is the data range large enough for appropriate static background selection and removal (see Fig. 9), especially if a static background is used?
  - Does the background appropriately match the spectrum or inappropriately intersect parts of the spectrum (as shown in Fig. 11)?
  - If endpoints have been selected for a static background, do they effectively average any general noise in the overal spectrum background? See, for example, Fig. 8.
  - Does the background model(s) appropriately deal with sloping backgrounds and overlapping or nearby peaks?
- Is the background model selected appropriate for application?
  - If compared to other spectra or used for quantitative analysis, is the background used the same or compatible with other analysis, including peak fitting, or the development of sensitivity factors used for quantitative analysis.[17,18]
  - Does the background cover the needed range to integrate the signals for quantitative or other analysis (e.g., Fig. 9.).
  - Do the results extracted after background removal make physical and chemical sense? Does the quantification of peak intensities give sensible compositional results? If the same approach is applied to reference material, does the approach give expected results? Do relative peak intensities fit with the physics and chemistry of the sample?
  - The background described by the Tourgaard approach is present to different degrees in all samples. Particually, if an active approach or fitting is being done, have these loss electrons been appropriately considered?

Downloaded from http://pubs.aip.org/avs/jva/article-pdf/doi/10.1116/6.0000359/15821876/063203_1_online.pdf

Published under license by AVS.

VI. SUMMARY AND CONCLUSIONS

Consideration, identification, and removal or incorporation of background signals are essential components of XPS data analysis. Signal strengths need to be separated from background signals for quantitative analysis and the background model applied will impact relative signal strengths during peak fitting processes. Fundamental aspects of the backgrounds in XPS spectra are not understood and subject to ongoing research. The results of such research will likely both increase mechanistic understanding and improve quantitative aspects of XPS analysis.

Because there are multiple approaches to the type and use of backgrounds in analysis, it is critical that the approaches used be well described to enable others to assess and/or apply similar analyses. Similarly, when spectra are displayed it is important that the background be included in the relevant figures.

Although there may be no ideal or totally correct background, many common damaging errors appear in the literature. Many of the most common errors have been identified and described in this guide including inappropriate background selection, inappropriate end point selection, too small data collection range, not including background information in reported results, and not showing the background in spectrum fits.

Whatever approach to background is selected, it is appropriate to assess the results in the context of the information desired, sensibility of the chemical and quantitative information obtained, and relationship to standards or reference material.

Although many users effectively remove the background from further analysis by what has been identified as the "static" approach, there are significant advantages, and some lessening of data requirements, to include a background in a fitting process (active approach).

ACKNOWLEDGMENTS

A portion of research was performed using EMSL (Grid. No. 436923.9), a DOE Office of Science User Facility sponsored by the Office of Biological and Environmental Research.

APPENDIX A: IMPACT OF SATELLITE PEAKS ON O 1 S PEAK INTENSITY DETERMINATION: CHALLENGES RELATED TO TiO_2

This appendix focuses attention on the O 1 s spectrum and has two parts. The first part demonstrates by example the nature and significant amount of satellite intensity in O 1 s signals from the TiO_2 used earlier and for a cerium oxide sample. As shown below, the presence of adjacent Ti peaks complicates truly accurate determination of O 1 s satellite intensity for TiO_2. The second part of the appendix shows both reasonable and more problematic approaches for getting an approximate O 1 s intensity from the TiO_2 without peak fitting that necessarily misses part of the satellite signals. When removing backgrounds for quantitative analysis it is important to know about and consider the presence and possible impacts of satellite peaks and, of course, to appropriately describe the approach that has been used and the approximations and assumptions applied.

The importance and significance of satellite peaks was highlighted in Fig. 6 in Sec. II B. As noted in Sec. IV B, these peaks were often not collected or highlighted in some of the important and useful earlier TiO_2 and other data.[56,57] Significant satellite peaks are present for both the Ti 2p and O 1 s photoelectron peaks for the sample used in the examples in this paper. Our understanding of the amount of signal intensity associated with these peaks has increased over time along with the instrument advances that enable analysts to measure them more clearly. It is important for the analysts to recognize that satellite peaks may well be present and contain significant signal intensity. These signal intensities should, in principle, be used during in quantification. Area ratios based upon only the areas under the principal peaks in two regions (e.g., Ti 2p and O 1 s) may give an appropriate intensity ratio without having to take into account intensity from satellites if the percentage of the intensity in satellites in the two regions is comparable (which might or might not be a fortuitous circumstance) or if appropriate sensitivity factors (for similar materials with similar peak structures) were determined from reference samples without including satellites. Obtaining percentage composition based upon area ratios is a process that involves several assumptions and careful attention is required if exact quantification is required. Such challenges and required assumptions highlight the need for a systematic consistent approach, the use of reference materials, and reporting of the approach and analysis details. Many of these issues as related to quantitative analysis are discussed in this collection of papers by Brundle and Crist[17] and Shard.[18]

Satellite peaks can, in various samples, often be found at slightly higher and sometimes significantly higher binding energies (even as much as 50 eV) than the principal peak, therefore, it is advisable to check for such peaks before analysis. Of course, satellites at much higher binding energies might overlap with other principal photoelectron peaks, complicating analysis. Figure 19 shows the extended O 1 s region (84 eV wide) for TiO_2 and CeO_2. In the case of CeO_2 [Fig. 19(b)], there are no overlapping photoelectron peaks in this wide 84 eV region. Extensive satellite features can be seen and based on background and peak fits described below, Table VII shows that only 66.8% of the intensity is contained in the principal O 1 s features due to oxide and a small amount of hydroxide. The analyst seeking to use the O 1 s peak area for quantification needs to be aware of the 33.2% intensity in the extended satellite region. In the case of TiO_2 [Fig. 19(a)], there is overlap between the O 1 s satellite region and the Ti 2 s region. The features at higher binding energies than Ti 2 s are probably satellites from the principal Ti 2 s peak, though satellites from the O 1 s region may overlap this region so the first three peaks in Table VII may contain O 1 s satellite intensity. If one takes the five peaks in the table marked as O 1 s satellites, then Table VII shows that only 56.4% of the intensity is contained in the principal O 1 s features due to oxide and a small amount of hydroxide and perhaps chemisorbed oxygen. Once again, the analyst seeking to use the O 1 s peak area for quantification needs to be aware of the at least 43.6% intensity in the extended satellite region. This percentage might be greater if some O 1 s satellite intensity overlaps with the Ti 2 s region and its associated satellites. In the two peak fits in Fig. 19, true Voigt functions and an iterative Shirley background was used. However, the iterative Shirley background was

Downloaded from http://pubs.aip.org/avs/jva/article-pdf/doi/10.1116/6.0000359/15821876/063203_1_online.pdf

Published under license by AVS.

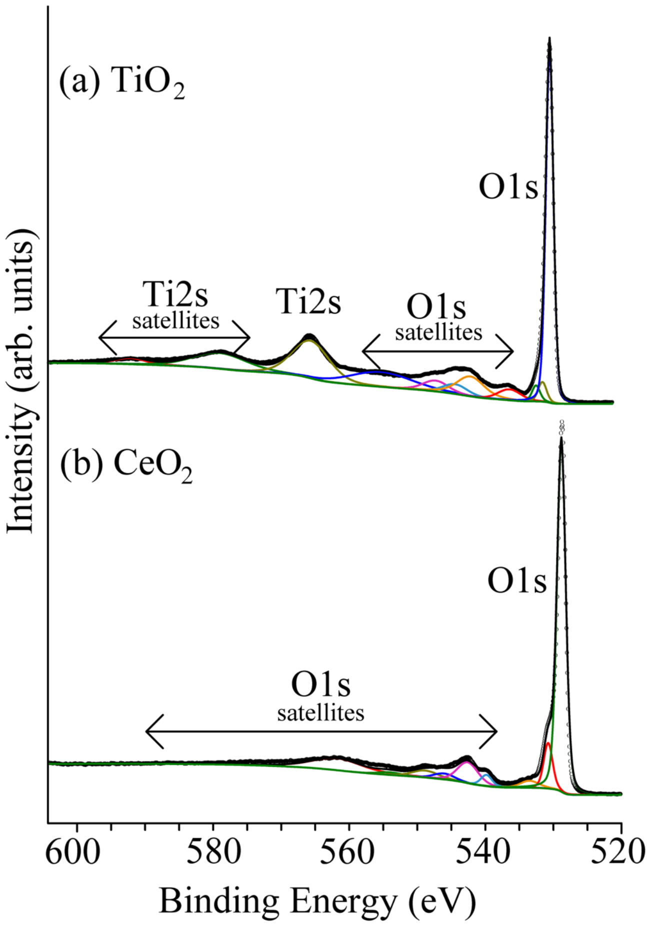

FIG. 19. XPS wide scan of the O 1s region of (a) TiO_2 and (b) CeO_2. In the case of TiO_2, the Ti 2s region and its associated satellites overlap with the O 1s satellite region. The spectra were obtained with monochromatic AlKα X-radiation. Fitting details are given in Table VII.

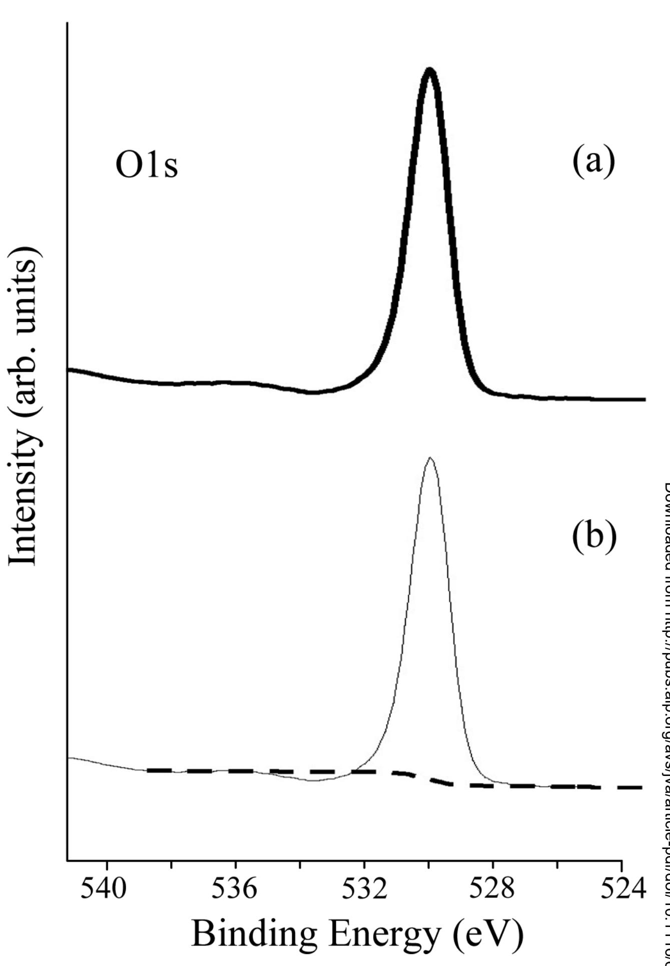

FIG. 20. XPS scan of the O 1s region of TiO_2 shown in (a) shows one of the satellite features at 535.6 eV. The dotted line in (b) shows how an iterative Shirley background in this spectral range comes above the experimental data around 534 eV.

split into two parts. The iterative process allowed the position of the background at the beginning and the end of the spectral region to vary, but a fixed point was set (binding energy and counts) at 533.5 eV for TiO_2 and 536.8 eV for CeO_2. Essentially there are two iterative Shirley backgrounds in these active fits. It is important to point out that the fits in Fig. 19 use the minimum number of peaks to fit the peak envelope. Theoretical calculations of satellite features often show a large number of components and indeed it would be possible to fit these spectra with more component peaks. The purpose of the fits are not to show definitively all the many possible and overlapping satellite features (as multiple overlapping peaks cannot be distinguished in the experimental data from single peaks) but to indicate where the principal peaks (or clusters of overlapping peaks) lie and to evaluate the overall intensity arising from satellites. As with all curve fits these fits are not unique and the relative intensity of the satellite features will change if the background model is changed.

The anatase TiO_2 data discussed in Secs. IV B and IV C 1 include the use of the O 1 s signal intensity. Even in a relatively narrow scan of the O 1 s region in Fig. 20, it is appropriate to include the satellite peak at 535.6 eV (as has been done in Fig. 19). Higher energy peaks, often associated with OH, water or some type of defects are often observed in O 1 s spectra for TiO_2. In this case, as the nanoparticle sample had been heated in O_2, oxygen may be incorporated in some way with the particles; it might be appropriate to include this oxygen signal in the analysis. The fit in Fig. 19 includes two O 1 s peaks attributed to these other oxygen species.

In the narrow O 1 s region, most of the signal intensity resides in the main 1 s peak centered around 530 eV. If the analyst wanted to include the satellite peak at 535.6 eV, it might be assumed that an iterative Shirley background might be appropriate. However, the higher background above 540 eV causes the iterative Shirley background to inappropriately cut across the spectrum. The Smart

Downloaded from http://pubs.aip.org/avs/jva/article-pdf/doi/10.1116/6.0000359/15821876/063203_1_online.pdf

Published under license by AVS.

background is designed to avoid such crossings, but in this case gives an unreasonable result. Figure 20(b) shows how the iterative Shirley background comes above the experimental data. Using an iterative Shirley background separately in the manner described above used to fit the data in Fig. 19 for the main and satellite peaks gives the relative intensities shown in Table VII. In the results shown in Tables III and V for O 1 s intensity and the Ti/O atom ratios, the intensity of the first satellite peak has been included. The percentage differences are not large for the first satellite peak at 535.6 eV but are substantial when all the satellite features are included. As stated above, ignoring a large part of the satellite intensity in quantitative analysis may work if the analyst is lucky (there is roughly the same percent of signal intensity for all of the peaks involved thus not impacting peak intensity ratios) or the sensitivity factors used were derived from reference materials with similar peak structures and satellite intensities and the satellite features were not included in the reference signal intensities.

APPENDIX B: GREATER COMPLICATION WHEN ACHROMATIC RADIATION IS USED AND THE IMPACT OF FITTING FUNCTION AND COMPONENT PEAKS

In the case of spectra obtained with achromatic x-radiation, the analysis needs to include photoelectron peaks that have been generated by the various x-ray satellites. X-ray satellites lead to each component peak being represented by separate peaks corresponding to photoelectrons ejected by $K\alpha_{1,2}$, $K\alpha'$, $K\alpha_3$, $K\alpha_4$, $K\alpha_5$, $K\alpha_6$, and K_β X-rays. In the narrow energy ranges typically analyzed by curve fitting, nearly all the X-ray intensity comes from the $K\alpha_{1,2}$ X-rays, but the additional peaks generated in particular by the $K\alpha'$, $K\alpha_3$, and $K\alpha_4$ X-radiation are sufficiently intense to require inclusion in the background determination and the analysis of the spectral features. For examples including these satellite peaks, see Sherwood.[9]

Consider the spectrum for oxidized tungsten using achromatic x-radiation reported previously[10] shown in Fig. 15. The W4f spectrum of metallic tungsten with a surface oxidized layer obtained with MgKα achromatic x-radiation are shown fitted to spin–orbit split peaks for the metal and oxidized tungsten using different background models and Gaussian/Lorentzian product functions with an exponential tail.[61] The results of an active approach where an iterative Shirley background was included in the fit is shown in Fig. 15(a).

This means that the parameters for the iterative background (the high and low binding energy background values) together with the seven parameters which define each peak (so for the four peaks in the figure this represents 28 parameters) are allowed to vary in the iterative nonlinear least squares curve fitting process.[9]

The experimental data can be compared with the fitted envelope containing the fitted peaks and the background using the statistical chi-squared (χ^2). This is defined in this paper as

$$\chi^2 = \sum_{r=1}^{N} w_r [y_r - F(x_r|\mathbf{q})]^2, \quad \text{(B1)}$$

where $F(x|\mathbf{q})$ is the fitting function and y_r represents the observed counts at a given value of $x = x_r$. N represents the total number of points in the spectrum and w_r is a weighting function which when chosen as y_r^{-1} makes χ^2 equal to the statistical chi-square. The reduced χ^2 is defined as the χ^2 value divided by (number of data points − the number of independent parameters in the fitting function). The lowest chi-squared value is usually, but not always, indicative of the best fit. Table VI shows the χ^2 values for the fits using different fitting and background models, with good fits characterized by low values of χ^2 and a good visual appearance of the fit.

This appendix will discuss in more detail the background and fitting considerations in the tungsten example presented in Figs. 15–17 and Table VI. The relatively poor performance of the "static" approach in the tungsten example in Fig. 15 illustrates how the removal of the background from the experimental data before fitting requires the user to select the correct background parameters. It is clear from Fig. 15(a) that the "active" approach finds that the correct background at the low binding energy side of the spectrum lies substantially below the data points at binding energies below 30 eV. In this example, it is the presence of intensity from the photoelectron peaks excited by $K\alpha_3$, $K\alpha_4$ x-rays from the $W4f_{3/2}$ peak of the oxidized tungsten that is positioned below 30 eV that causes difficulties in correctly selecting the starting point for background subraction in the "static" approach.

The active fit in Fig. 15 gave the best fit in terms of the appearance of the fit and the lowest χ^2 value. It is important to ask whether this fit makes the most scientific sense. Both the relevance of the parameters applied to fitting of the W photoelectron peaks and the nature of the background used can impact the quality of the scientific information obtained. These issues were examined in Figs. 16 and 17, respectively.

In this example, it would be relevant to start with information about the fitting parameters for the oxidized tungsten and tungsten metal. These fitting parameters will allow the function parameters for the potential components to be determined for the chosen fitting function using experimental information for the same instrument. This is because peak shapes can vary from instrument to instrument. In Fig. 17, a Gaussian/Lorentzian product function was used with a Gaussian/Lorentzian mixing ratio of 0.5 and an exponential tail slope of 0.032 for the W4f metal peaks.[61] These were the values used previously.[10] A number of questions arise with the active fit in Fig. 15:

- The metal peaks would be expected to have more Lorentzian than Gaussian character.
- Conduction band interaction on conducting species can be represented in a number of ways including an exponential tail. The exponential tail on the metal peaks in Fig. 15(a) is substantial—could there be intensity due to one or more additional oxidized tungsten species and a smaller exponential tail?
- How might the fit appear if the spectrum is fitted using a more scientifically correct true Voigt function.

The first point can be addressed by refitting the spectrum using peaks with more Lorentzian character for the metal peaks. The fitting of the data in *eSpectra*®[64] for the metal[65] yields an exponential tail on the metal that should be 0.07 and not 0.032 as for the experimental data in Fig. 15. The *eSpectra*® data also show the presence of a W 5p peak with significant intensity that was missing in

Downloaded from http://pubs.aip.org/avs/jva/article-pdf/doi/10.1116/6.0000359/15821876/063203_1_online.pdf

Published under license by AVS.

TABLE VII. Curve fitting information for TiO_2 and CeO_2.

TiO_2 Peak	Binding energy (eV)	Area as % of total areas	Voigt FWHM (eV)	Gaussian FWHM (eV)	Lorentzian FWHM (eV)
	Reduced $\chi^2 = 14.88$ 1345 data points (doubled from the original 673 data points)				
Ti2s[a]	591.29	2.66	5.23	3.72	2.50
Ti2s[a]	578.10	11.09	9.36	8.00	2.41
Ti2s	564.84	17.77	6.49	5.75	1.32
O1s[a]	554.45	11.97	10.57	8.77	3.15
O1s[a]	546.47	3.74	4.36	3.47	1.53
O1s[a]	543.63	3.25	4.20	3.29	1.56
O1s[a]	541.37	7.71	4.77	3.50	2.12
O1s[a]	535.60	3.21	3.98	3.55	0.77
O1s[d]	531.74	1.76	1.39	1.10	0.50
O1s[c]	530.81	2.27	1.46	1.17	0.05
O1s[b]	529.71	34.57	1.39	1.25	0.25
CeO_2	Reduced $\chi^2 = 20.75$ 1345 data points (doubled from the original 673 data points)				
O1s[a]	561.67	12.59	8.84	6.23	4.30
O1s[a]	553.84	1.06	3.81	3.53	0.51
O1s[a]	548.66	3.49	4.44	3.70	1.29
O1s[a]	545.88	2.26	3.56	3.04	0.91
O1s[a]	542.38	8.34	3.61	3.01	1.04
O1s[a]	539.63	2.47	2.00	1.67	0.57
O1s[a]	533.33	2.85	3.30	2.21	1.75
O1s[c]	530.62	7.80	1.56	1.34	0.38
O1s[b]	528.63	59.04	1.59	1.37	0.37

[a]Satellite peak.
[b]Oxide.
[c]Hydroxide.
[d]Chemisorbed water/oxygen.

Fig. 15. When the data in Fig. 15 are refitted to address these points, the "active" approach fits in Fig. 16 are obtained. Figure 16 uses an iterative Shirley background[10] included in the fit. In Fig. 16(a), the Gaussian/Lorentzian product function has more Lorentzian character (Gaussian/Lorentzian mix of 0.85) and an exponential tail of 0.07 on the metal peaks In Fig. 16(b), true Voigt functions are used[50] to fit the spectrum with a *glmix* (Gaussian/Lorentzian mix in the Voigt function) of 0.09 for the oxidized tungsten species and 0.60 for the metal. In both cases, a W 5p feature was included in the fit as well as an additional oxidized tungsten species. The fitting information is shown in Table VI. Both fits are reasonable but the total fitted area and the relative amounts of tungsten species varies. This is caused by difference in the fitting function including the relative amounts of Gaussian and Lorentzian character. No curve fit is unique but this example illustrates how the choice of fitting function and component peaks can impact the determination of the amount of species present. To the extent possible, it is important to be consistent in the approach to background use and fitting approach, including appropriate available relevant physical and chemical information.

The impact of the choice of background model on the relative amount of species present can be illustrated by using an "active" fit with an iterative Shirley background using the same Voigt function parameters that were used in Fig. 16, but changing the background model included in the iterative process. The results of these fits are shown in Fig. 17 and Table VI. The best quality fit occurs with the iterative Shirley background, but the most striking difference is in the amount of species present when a Tougaard background is used.[29] The use of a Tougaard background leads to a 16.3% increase in the total fitted area compared to the iterative Shirley background as well as the need to add another tungsten species (WO_2) to the fit.

As noted earlier, these and other fits are not unique, but the examples in this section illustrate the impact that the choice of background and other peak properties can have on the determination of the amount of species present. As noted in Appendix A, throughout this paper, it is important to present the assumptions and approach in data records and published reports. Known physical and chemical information should be considered in the background removal and fitting process.

REFERENCES

[1]J. F. Watts and J. Wolstenholme, *An Introduction to Surface Analysis by XPS and AES* (Wiley, Chichester, 2003), pp. 40–44.
[2]M. A. Rooke and P. M. A. Sherwood, Surf. Interface Anal. **21**, 681 (1994).
[3]T. Dickinson, A. F. Povey, and P. M. A. Sherwood, J. Electron Spectrosc. Relat. Phenom. **2**, 441 (1973).

Downloaded from http://pubs.aip.org/avs/jva/article-pdf/doi/10.1116/6.0000359/15821876/063203_1_online.pdf

Published under license by AVS.

[4]A. Herrera-Gomez *et al.* Surf. Interface Anal. **50**, 246 (2018).
[5]A. Herrera-Gomez, The active background method in XPS data peak fitting, CINVESTAV—Queretaro, Internal Report 2012, see: http://www.qro.cinvestav.mx/~aherrera/reportesInternos/activeBackground.pdf.
[6]S. Tougaard, Surf. Sci. **162**, 875 (1985).
[7]S. Tougaard, Surf. Interface Anal. **50**, 657 (2018).
[8]A. Herrera-Gomez, M. Bravo-Sanchez, O. Ceballos-Sanchez, and M. O. Vazquez-Lepe, Surf. Interface Anal. **46**, 897 (2014).
[9]P. M. A. Sherwood, Surf. Interface Anal. **51**, 589 (2019).
[10]A. Proctor and P. M. A. Sherwood, Anal. Chem. **54**, 13 (1982).
[11]ISO Technical Report 18392:2013, Surface chemical analysis—X-ray photoelectron spectroscopy—Procedures for determining backgrounds (unpublished).
[12]ASTM International, *E995 Guide for Background Substraction Techniques in Auger Electron and X-ray Photoelectron Spectroscopy* (ASTM International, West Conshohocken, PA, 2016).
[13]N. Farley, Casa Software Ltd. www.casaxps.com (2006), see: http://www.casaxps.com/help_manual/manual_updates/peak_fitting_in_xps.pdf, Vol. 2020.
[14]H. E. Bishop, Surf. Interface Anal. **3**, 272 (1981).
[15]N. Fairly, in *Surface Analysis by Auger and X-ray Photoelectron Spectroscopy*, edited by D. Briggs and J. T. Grant (I. M. Publications, Chichester, 2003), p. 398.
[16]C. Jansson *et al.*, Surf. Interface Anal. **23**, 484 (1995).
[17]C. R. Brundle and B. V. Crist, J. Vac. Sci. Technol. A **380**, 41001 (2020).
[18]A. G. Shard, J. Vac. Sci. Technol. A **31**, 041201 (2020).
[19]G. H. Major, N. Farley, P. M. A. Sherwood, M. R. Linford, J. Terry, V. Fernandez, and K. Artyushkova, "Practical guide for curve fitting in x-ray photoelectron spectroscopy," J. Vac. Sci. Technol. A (in press).
[20]A. Herrera-Gomez, J. Vac. Sci. Technol. A **38**, 033211 (2020).
[21]C. D. Easton, C. Kinnear, S. L. McArthur, and T. R. Gengenbach, J. Vac. Sci. Technol. A **38**, 023207 (2020).
[22]D. R. Baer, J. Vac. Sci. Technol. A **38**, 031201 (2020).
[23]T. Conard, A. Vanleenhove, and P. V. D. Heide, J. Vac. Sci. Technol. A **38**, 033206 (2020).
[24]J. F. Moulder, W. F. Stickle, S. P. E. and K, and D. Bomben, *Handbook of X-Ray Photoelectron Spectroscopy* (Perkin-Elmer, Eden Prairie, MN, 1992).
[25]D. R. Baer and A. G. Shard, J. Vac. Sci. Technol. A **38**, 031203 (2020).
[26]M. C. Biesinger, L. W. M. Lau, A. R. Gerson, and R. S. C. Smart, Appl. Surf. Sci. **257**, 887 (2010).
[27]S. Thomas, P. M. A. Sherwood, N. Singh, A. Al-Sharif, and M. J. O'Shea, Phys. Rev. B **39**, 6640 (1989).
[28]S. Tougaard, J. Vac. Sci. Technol. A **5**, 1230 (1987).
[29]S. Tougaard and P. Sigmund, Phys. Rev. B **25**, 4452 (1982).
[30]D. Briggs and M. P. Seah, *Practical Surface Analysis: Auger and X-ray Photoelectron Spectroscopy* (Wiley and Sons, New York, NY, 1990), Vol. 1, pp. 233–239, 555–586.
[31]D. A. Shirley, Phys. Rev. B **5**, 4709 (1972).
[32]A. M. Salvia and J. E. Castle, J. Electron Specrosc. **95**, 45 (1998).
[33]J. E. Castle and A. M. Salvi, J. Vac. Sci. Technol. A **19**, 1170 (2001).
[34]J. Vegh, J. Electron Specrosc. **46**, 411 (1988).
[35]E. N. Sickafus, Phys. Rev. B **16**, 1436 (1977).
[36]S. Tougaard, Surf. Interface Anal. **25**, 137 (1997).
[37]R. Hesse, M. Weiß, R. Szargan, P. Streubel, and R. Denecke, J. Electron Specrosc. **205**, 29 (2015).
[38]W. S. M. Werner, Surf. Interface Anal. **23**, 737 (1995).
[39]J. Vegh, Surf. Interface Anal. **20**, 860 (1993).
[40]N. Pauly, F. Yubero, J. P. Espinós, and S. Tougaard, Surf. Interface Anal. **51**, 353 (2019).
[41]M. C. Biesinger, B. P. Payne, L. W. M. Lau, A. Gerson, and R. S. C. Smart, Surf. Interface Anal. **41**, 324 (2009).
[42]D. Cabrera-German, G. Molar-Velázquez, G. Gómez-Sosa, W. de la Cruz, and A. Herrera-Gomez, Surf. Interface Anal. **49**, 1078 (2017).
[43]P. M. A. Sherwood, J. Vac. Sci. Technol. A **14**, 1424 (1996).
[44]S. Tougaard, Solid State Commun. **61**, 547 (1987).
[45]A. Herrera-Gomez, M. Bravo-Sanchez, F. S. Aguirre-Tostado, and M. O. Vazquez-Lepe, J. Electron Specrosc. **189**, 76 (2013).
[46]S. Tougaard, Surf. Interface Anal. **26**, 249 (1998).
[47]A. Müller *et al.*, J. Phys. Chem. C **123:49**, 29765 (2019).
[48]S. Tougaard, Users guide QUASES-Tougaard quantitative analysis of surfaces by electron spectroscopy version 5.1, QUASES Tougaard ApS, Odense SO, Denmark, 2011, see: http://www.quases.com/data/documents/QUASES-Tougaard=20Ver5=20Manual.pdf.
[49]S. Tougaard, "Practical guide to the use of backgrounds in quantitative XPS," J. Vac. Sci. Technol. A (submitted).
[50]P. M. A. Sherwood, Surf. Interface Anal. **51**, 254 (2019).
[51]A. Herrera-Gomez, AAnalyzer: A peak-fitting program for photoemission data, see: http://rdataa.com/aanalyzer/aanaHome.htm.
[52]S. Tougaard, Surf. Sci. **216**, 343 (1989).
[53]See PHI Multipak Software for https://www.ulvac-phi.com/en/products/database-books/phi-multipak/.
[54]M. H. Engelhard, D. R. Baer, and L. Chen, "XPS data from lightly Pd doped TiO2 anatase nanoparticles," Surf. Sci. Spectra (submitted).
[55]A. E. Bocquet, T. Mizokawa, K. Morikawa, A. Fujimori, S. R. Barman, K. Maiti, D. D. Sarma, Y. Tokura, and M. Onoda, Phys. Rev. B **53**, 1161 (1996).
[56]D. Barreca, A. Gasparotto, C. Maccato, C. Maragno, and E. Tondello, Surf. Sci. Spectra **14**, 27 (2007).
[57]U. Diebold and T. E. Madey, Surf. Sci. Spectra **4**, 227 (1996).
[58]J. H. Scofield, J. Electron Spectrosc. Relat. Phenom. **8**, 129 (1976).
[59]. S. Bagus, C. J. Nelin, C. R. Brundle, and S. A. Chambers, J. Phys. Chem. C **123**, 7705 (2019).
[60]J. J. Olivero and R. L. Longbothum, J. Quant. Spectrosc. Radiat. Transfer **17**, 233 (1977).
[61]R. O. Ansell, T. Dickinson, A. F. Povey, and P. M. A. Sherwood, J. Electroanal. Chem. Interfacial Electrochem. **98**, 79 (1979).
[62]P. M. A. Sherwood, in *Surface Analysis by Auger and X-Ray Photoelectron Spectroscopy*, edited by D. Briggs and J. T. Grant (SurfaceSpectra, Chichester, 2003), pp. 531–555.
[63]P. M. A. Sherwood, J. Vac. Sci. Technol. A **15**, 520 (1997).
[64]*eSpectra*, AIP Spectral Data System, see: https://espectra.aip.org/app/#/home, Vol. 2020.
[65]M. H. Engelhard and D. R. Baer, Surf. Sci. Spectra **7**, 1 (2000).

Downloaded from http://pubs.aip.org/avs/jva/article-pdf/doi/10.1116/6.0000359/15821876/063203_1_online.pdf

Published under license by AVS.